DOI:10.14753/SE.2014.1917

Prognostic impact of DNA ploidy and protein expression of enhancer of zeste homologue 2 (EZH2) in synovial sarcoma

PhD thesis

Dr. Yi-Che William Chang Chien

Pathological Sciences Doctoral School
Semmelweis University

Supervisor: Dr. Zoltán Sápi M.D., Ph.D., D.Sc., professor

Official reviewers:
Dr. Erika Tóth M.D., Ph.D., consultant pathologist
Dr. Tamás Terebessy M.D., Ph.D., lecturer

Head of the final examination committee:
Dr. Zsuzsa Schaff M.D., Ph.D., D.Sc., professor

Members of the final examination committee:
Dr. Áron Lazáry M.D., Ph.D., research and development manager
Dr. Katalin Borka M.D., Ph.D., assistant professor

Budapest, 2013

DOI:10.14753/SE.2014.1917

Table of Contents

DOI:10.14753/SE.2014.1917

DOI:10.14753/SE.2014.1917

The list of Abbreviation

- BPSS, Biphasic synovial sarcoma
- CDK1, cyclin dependent kinase 1
- Dc, Complex dipoid
- DCC, deleted in colorectal cancer
- DI, DNA index
- DNMT, DNA Methyltransferase
- DOG-1, discovered on GIST-1
- Ds, Simple diploid
- DZNep, 3-deazaneplanocin
- EED, embryonic ectoderm development
- EGR1, early growth response 1
- EZH2, Enhancer of zeste homologue 2
- FFPE, formalin-fixed and paraffin embedded
- FGFR2, fibroblast growth factor receptor 2
- FISH, Fluorescence in situ hybridization
- GIST, gastrointestinal stromal tumor
- H3K27me3, Trimethyl-histone H3 (Lys27)
- HAT, histone acetyltransferase
- HDAC, Histone deacetylase
- HR-CGH, High resolution-comparative genomic hybridization
- IOD, Integrated optical density
- JARID2, jumonji, AT rich interactive domain 2
- KRAB, Kruppel-associated box

- LHX4, LIM-homeobox protein
- lincRNA, large interventing noncoding RNA
- MPSS, Monophasic synovial sarcoma
- PcG, Polycomb group
- PDSS, Poorly differentiated synovial sarcoma
- PRC, Polycomb repressor complex
- qRT-PCR, Quantitative real time- polymerase chain reaction
- SCI, single cell interpretation
- SH2-binding motifs, Src homology 2 binding motif
- SH3-binding motifs (Src homology 3 binding motif
- siRNA, Small interfering RNA
- SLI, stemline interpretation
- SNH, SYT N-terminal homology
- SS, Synovial sarcoma
- SSXRD, SSX repressive domain
- SUZ12, suppressor of zeste 12
- TF, transcription factors
- TLE1, transducer-like enhancer of split 1
- UTR, untranslated region
- VEGF, vascular endothelial growth factor
- YY1, Yin-Yang 1

DOI:10.14753/SE.2014.1917

I. Introduction

I.1 Clinical findings

Synovial sarcoma, an aggressive soft tissue tumor with high rate of local recurrence and distant metastasis is currently hypothesized to originate from mesenchymal stem cells [1]. It occurs most commonly in young patients, representing about 10% of soft tissue sarcomas in all age groups and about 15-20% in adolescents. It is most prevalent in adolescents and young adults between 15 and 40 years of age with mean age of 34 years. 40% of them were under age 30 when diagnosis was made. Males are affected slightly more often than females (1.2:1). Despite the name, synovial sarcomas do not arise from or differentiate toward the synovium; they are extremely rare to be found within the joint cavities; with more than 80% of the cases arising in deep soft tissues around large joints or tendons [2]. However, any body part, including retroperitoneum, mediastinum, thoracic wall, head and neck region even visceral organs cannot be spared from this tumor indicating non-synovial origin; hence, the traditional term ‘synovial’ is a misnomer. The most common presentation is a palpable, deep-seated swelling mass with or without pain, mild movement limitation can be encountered. The clinical progression is usually slow and sometimes may be ignored the malignant nature of the tumor and consequently delay the diagnosis and therapy. Additionally, the clinical differential diagnosis can be hematoma, arthritis or bursitis. Few studies have reported synovial sarcoma arising from the field of previous therapeutic irradiation and the site of prosthesis implantation [3, 4]. The characteristic radiological finding is the presence of multiple small radiopacities representing calcification or, rarely, ossification which can be found approximately 15~20% of the

DOI:10.14753/SE.2014.1917

cases **(Figure 1)**. Computed tomography can be used to assess the involvement and extension of the tumor.

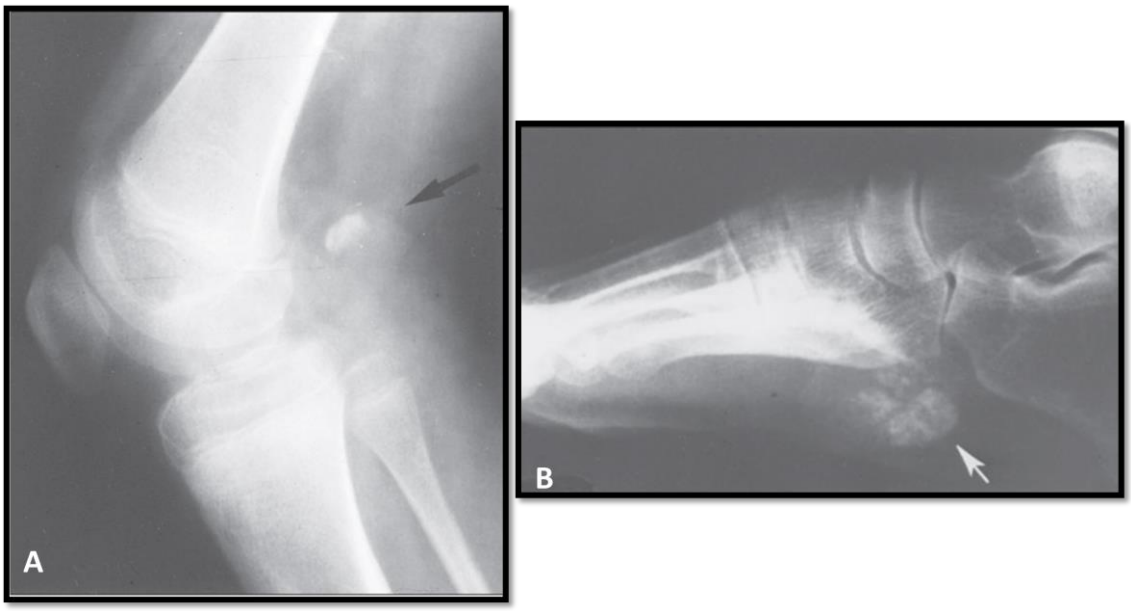

Figure 1. Synovial sarcoma originating in **(A)** popliteal fossa and **(B)** plantar region with calcification [5].

I.2 Pathology features

Grossly when slow growing, the lesion usually has circumscribed, lobular border with compressing the adjacent tissue. Cystic change and calcification can be found. In some cases, especially poorly differentiated subtype, fast growth can be expected, usually with fleshy, variegated surface and shaggy border; frequently with areas of hemorrhage and necrosis **(Figure 2)**.

DOI:10.14753/SE.2014.1917

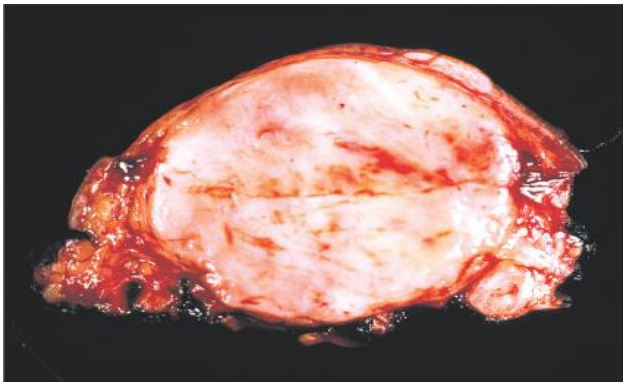

Figure 2. Gross feature of poorly differentiated synovial sarcoma with fleshy cut-surface and focal hemorrhage.

Histologically, synovial sarcomas are composed of 2 unique cellular components: spindle cells and epithelioid cells with varying proportions. Morphologically, they can display biphasic (BPSS) monophasic (MPSS), and poorly differentiated (PDSS) patterns **(Figure 3)** among which, MPSS can also be divided into monophasic fibrous and monophasic epithelial, respectively representing two extremes of morphologic spectrum of BPSS.

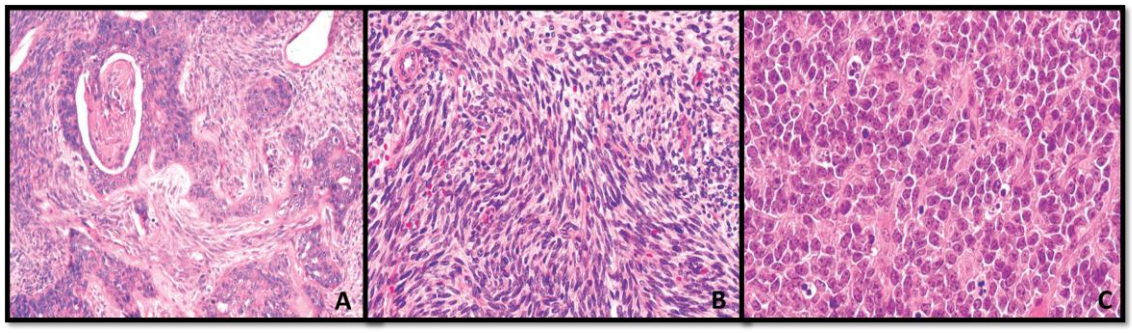

Figure 3. Histology of **(A)** biphasic, **(B)** monophasic and **(C)** poorly differentiated subtypes of synovial sarcoma.

The epithelioid component can have glandular, solid and papillary pattern and the spindle component usually has fascicular configuration. The BPSS and MPSS usually show bland nuclei and scanty mitotic activity. The background can show hyalinized or myxoid changes, calcification and mast cells can be numerous. PDSS, which accounts

DOI:10.14753/SE.2014.1917

for approximately 10% of all cases, is defined by high cellularity, high nuclear grade, and high mitotic activity, as well as areas of necrosis. Its morphology is typically dominated by small round cells or rhabdoid-like cells similar to undifferentiated embryonic cells, and its clinical course tends to be aggressive with early recurrence and metastasis [2, 5].

I.3 Immunophenotype and differential diagnosis

Both epithelioid and focal spindle components of synovial sarcomas show cytokeratin positivity, particularly CK7 and 19; additionally EMA, BCL-2, CD99 and S-100 protein may also show focal positivity although none of them is specific. A novel marker: transducer-like enhancer of split 1 (TLE1), a member of the *TLE* gene family encoding a transcriptional corepressor in Wnt/ β-catenin signaling pathway, which is necessary for epithelial and neuronal differentiation, has been found in gene expression profiling studies to be significantly overexpressed in synovial sarcomas [6]. In 91 out of 94 molecularly confirmed synovial sarcomas showed intranuclear positivity by immunohistochemical detection, therefore, it can serve as a useful diagnostic marker [6].

Due to its ubiquitous presence and the morphology resemblance of other much more common spindle cell tumors or carcinomas; the diagnosis of synovial sarcoma can be challenging; especially those within the retroperitoneal region and gastrointestinal tract; the differential diagnosis is wide. Mainly, gastrointestinal stromal tumor (GIST), myogenic tumors, solitary fibrous tumor, inflammatory myofibroblastic tumor, and neurogenic tumor should be considered. Probably the most important differential diagnosis is GIST, especially CD117-negative cases, since it shares morphological similarities with synovial sarcoma. Membranous or intracytoplasmic “discovered on GIST-1” (DOG-1) positivity in the former and diffuse intranuclear TLE1 positivity in the latter should tell the difference. Blunt ends and wavy nuclei with S-100 protein positivity are typical for neurogenic tumors; however, differentiating from malignant peripheral nerve sheath tumor (MPNST) can be challenging. Immunostaining for TLE1 and cytokeratin 7/19 can solve the difficult cases, since, according to the literature, the MPNST shows only focal weak TLE1 positivity instead of diffuse and strong ones seen

in synovial sarcoma, and it is usually cytokeratin 7/19 negative [7]. Focal area staghorn vascular structures may simulate a solitary fibrous tumor. CD34 is usually negative in synovial sarcoma. Interpreting the results with caution is important to avoid the diagnostic pitfalls, for example, mast cells within the synovial sarcoma may positively stain for CD117. The characteristic immunophenotype of these tumors is summarized in **Table 1**.

Table 1. Immunophenotype of the most common spindle cell tumors in the abdominal cavity.

	Synovial sarcoma	GIST	IMT	Leiomyo sarcoma	SFT	Neurogenic tumors
CK/EMA	+	-	-	-	-	-
CD117	-	+	-	-	-	-
TLE1	+	-	-	-	-	-
h-Caldesmon	-	+/-	-	+	-	-
S100	+/-	+/-	-	-	+/-	+
SMA	+/-	+/-	+	+	-	-
CD34	-	+/-	-	-	+	-
DOG-1	-	+	-	-	-	-
ALK	-	-	+	-	-	-
Desmin	-	-	+	+	+/-	-

(GIST: gastrointestinal stromal tumor; IMT: inflammatory myofibroblastic pseudotumor; SFT: solitary fibrous tumor)

Of course exceptions occur; we have also reported a case of metastatic gastrointestinal synovial sarcoma with desmin positivity simulating myogenic tumor [8]. Therefore, the final diagnosis was established by fluorescence in situ hybridization (FISH), and real time-polymerase chain reaction (RT-PCR) to detect the tumor-specific t(X;18) translocation, which can be found in both epithelioid and spindle cell

components, which serve as gold standards for the confirmative diagnosis **(Figure 4)**.

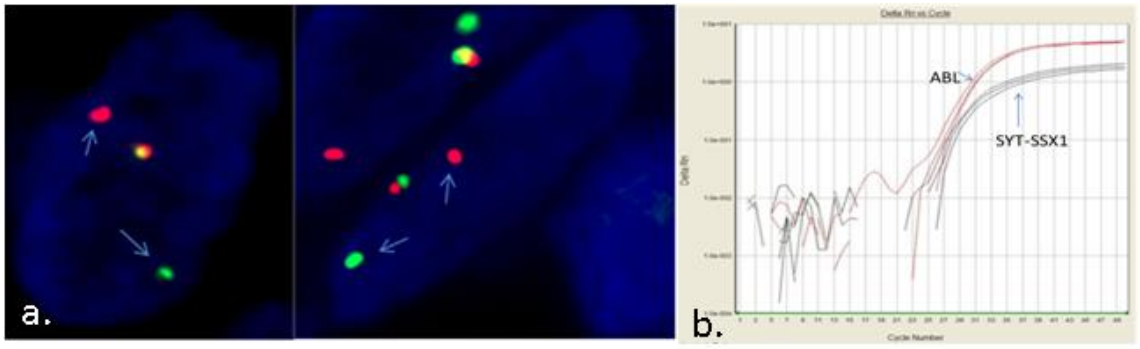

Figure 4. (a) Fluorescent in situ hybridization (FISH) contained mixture of probe labeled SYT gene. The arrows showed break apart of the gene indicating translocation. **(b)** Real-time PCR (RT-PCR) revealed the amplification of SYT-SSX1 gene (black), ABL gene (red) was used as internal control.

I.4 Cytogenetic characteristics

Synovial sarcoma is also a well-known "translocation-associated tumor" with characteristic balanced translocation between *SSX* located on chromosomes X and *SYT* on chromosome 18, t(X;18) (p11.2;q11.2), represented in more than 95% of the cases [9]. Due to their intranuclear locations and lack of DNA binding domains. SYT and SSX are thought to bind to other chromatin remodeling complexes or transcription factors to be transported in to nuclei where they exert their functions [10].

I.4.1 SYT protein functions as a transcriptional coactivator

The *SYT* gene, which is located on chromosome 18q11 and encodes a 387 amino acid protein, is ubiquitously expressed in human cells. It contains an SNH domain (SYT N-terminal homology domain) at the N-terminal region and interacts with SWI/SNF ATPase-associated chromatin remodeling complex (**Figure** 5) [11]. The SNH domain also interacts with transcription factors such as AF10, ATF2, histone acetyltransferase p300, and also histone deacetylase compressor SIN3A [12]. Their interactions with

SNH domain are mutually exclusive. However, the transcription factor such as AF10 alone can also directly interacts with SWI/SNF chromatin remodeling complex [13]. Therefore SYT, together with DNA binding proteins such as AF10, may exert its transcriptional coactivator function epigenetically through the recruitment of chromatin modification complexes such as SWI/SNF.

Additionally, the *SYT* gene also contains three SH2-binding motifs (Src homology 2 binding motif), one SH3-binding motif (Src homology 3 binding motif), and a C-terminal QPGY domain rich in glutamine, proline, glycine, and tyrosine [14]. The SH2-and SH3-binding motifs are thought to mediate protein-protein interactions in signal transduction whereas the QPGY domain was responsible for transcriptional activation [15].

I.4.2 SSX protein functions as transcriptional corepressor

In contrast to *SYT* gene, which is expressed ubiquitously, members of the *SSX* gene family, are immunogenic antigens expressed in testis and many malignant tumors, hence the name ‘‘cancer testis antigen”; although they can also been found in thyroid glands in low level as well [16].

The N-terminus of all SSX proteins exhibits extensive homology to the so-called “Kruppel-associated box” (KRAB) (**Figure 5**) which is involved in transcriptional repression [17]. In the C-terminus locates a stronger suppressive “SSX repression domain” (SSXRD) which shows high similarity across the SSX family [18]; while the 44 amino acid region immediately upstream of SSXRD exhibits high degree of diversity among the SSX family called divergent domain (DD) [18]. The SSXRD interacts with LIM-homeobox protein (LHX4), a transcription protein, and polycomb group complex (PcG) [19]. Therefore SSX, together with DNA binding proteins such as LHX4, may

exert its transcriptional corepressor function epigenetically through the recruitment of PcG-related chromatin modifiers.

I.4.3 SYT-SSX fusion protein in synovial sarcoma

The translocation juxtaposes the 5′-SYT (N-terminal) gene from chromosome 18 to either of three highly homologous genes at Xp11: 3′-SSX1, 3′-SSX2 or, rarely, 3′-SSX4 (C-terminal) [20, 21]. From a large sample analysis for the presence of SYT-SSX fusion; two thirds revealed an SYT-SSX1 fusion and one third an SYT-SSX2 [9] and only few cases showed SYT-SSX4 [22]. Since the SSX gene family encompasses at least 9 members, encoding 188 amino acid proteins with high degree of sequences homologies; the preference of SSX1, SSX2 and SSX4 fusion, instead of other members may due to not only the genomic architectural differences, but also the transforming potential of the encoded proteins [10, 23, 24].

The SYT-SSX fusion protein, which retains almost the entire SYT including entire SNH and most part QPGY domains, except the last eight amino acids, which are replaced by the last 78 amino acids of SSX containing SSXRD domain **(Figure 5**).

DOI:10.14753/SE.2014.1917

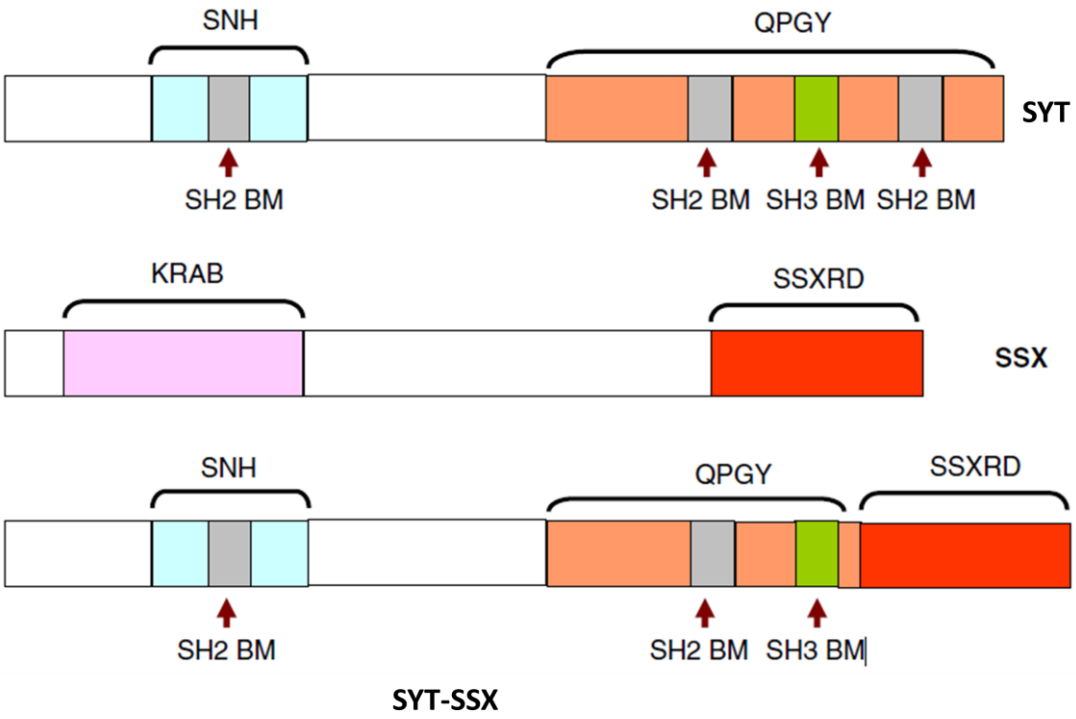

Figure 5. Proteins involved in synovial sarcoma t(X;18) translocation: the SYT-SSX fusion protein, which retains almost the entire (5′-end) SYT except the last eight amino acids, which are replaced by the last 78 amino acids of SSX (3′-end). (SNH: SYT N-terminal homology domain; QPGY: glutamine-, proline-, glycine-, and tyrosine-rich domain; SH2 BM: Src homology 2 binding motif; SH3 BM : Src homology 3 binding motif; KRAB: Kruppel-associated box; SSXRD: SSX repression domain) [25].

Due to their intranuclear localization and lack of a chromatin binding domain in both SYT and SSX proteins, this chimeric protein is thought to function as a transcriptional regulator modifying gene expression by associating with sequence-specific DNA-binding proteins mentioned before [9]. The predicted outcome is general alteration of cellular programming, both activation and silencing of target genes, once *SYT-SSX* is expressed. The bone marrow-derived mesenchymal stem cells and myoblasts transduced with *SYT-SSX* fusion gene showed high degree similarity of gene expression profiles with the synovial sarcoma cells such as *fgfr2*, a major inducer of neurogenesis during development [26] and knockdown of this gene abrogated the

growth in both transduced mesenchymal stem cells and synovial sarcoma cells and attenuated their neuronal phenotypes revealing the persistent effect of *SYT-SSX* function throughout the life of cancer [27].

Early literature has demonstrated that constitutive expression of human *SYT-SSX1* fusion gene in mouse fibroblast promoted growth rate in cell culture, increased anchorage-independent growth in soft agar, and formation of tumors with appearance similar to human synovial sarcoma when injected the transformed fibroblasts into nude mice indicated the oncogenic nature of SYT-SSX fusion protein although its oncogenic activity was reported to be much weaker compared with other traditional oncogene such as *RAS* [16]. Furthermore, lack of the N-terminal 181 amino acids of the fusion protein and overexpression of wild-type *SYT* alone were both fail to induce transformation in culture also imply that both *SYT*- and *SSX*- derived regions are needed for transformation [16]. It has also been shown that SYT-SSX fusion protein may suppress tumor suppressor genes such as *DCC* and *EGR1* which may partly contribute to the ongogenesis [16, 22]. It is widely accepted SYT-SSX fusion protein exerts its oncogenic property by epigenetically deregulating the target gene expression within the nucleus. Several studies using microarray-based transcriptional profiling and immunologic detection have revealed several possible target genes overexpressed as mRNA and protein levels by the fusion protein including growth factor such as IGF2 [28], growth factor receptors, components regulating cycle and survival such as Cyclin D1, BCL-2, EGFR, TLE and Her-2/neu and many others [29-32]. It has been documented that the SYT-SSX fusion protein up-regulated cyclin D1 protein level by inhibiting ubiquitin-dependent degradation and promoted proliferation [31]. However, the whole picture for the detailed molecular pathway deregulation is still under investigation.

I.4.4 Molecular biology of Enhancer of zeste homologue 2 (EZH2)

EZH2 is a member of the polycomb group (PcG) protein family which consists of epigenetic transcriptional repressors participating in cell cycle regulation, DNA damage repair, cell differentiation, senescence, and apoptosis [33].

PcG family members are arranged into multimeric polycomb repressive complexes (PRC), PRC1 and PRC2. EZH2 interacts with other units, "embryonic ectoderm development" (EED) and "suppressor of zeste 12" (SUZ12) to be functionally active and serve as the core members and catalytic units of PRC2. EZH2 acts as a histone methyltransferase through its SET domain and targeting the N-terminal tail of histone 3 and producing a characteristic trimethylated H3-Lys27 (H3K27me3) mark. It shows high expression in cells possessing embryonic gene expression signature, while its amount declines through maturation and differentiation [34, 35].

PRC2 can be recruited to the binding site of the target genes by PRC-associated transcription factors (e,g, YY1), DNA binding proteins (e.g. Jarid2), lincRNA or direct interaction with short transcripts produced from CpG islands [36-39]. H3K27me3 produced by PRC2 is recognized by PRC1 which, in turn, monoubiquitylates lysine 119 of histone H2A to prevent RNA polymerase II-dependent transcriptional elongation and lead to silencing of the downstream genes. However, recent data revealed a more complex mechanism of gene repression that PRC1 and PRC2 share similar but not entirely overlapping patterns of gene occupancy [40, 41], indicating a possibility of PRC2-independent PRC1 recruitment and gene repression.

PRC2 also interacts with other repressive epigenetic modifiers such as histone deacetylases (HDAC) and DNA methyltransferases (DNMT), which further promote chromatin condensation. **(Figure 6)** [42-44].

DOI:10.14753/SE.2014.1917

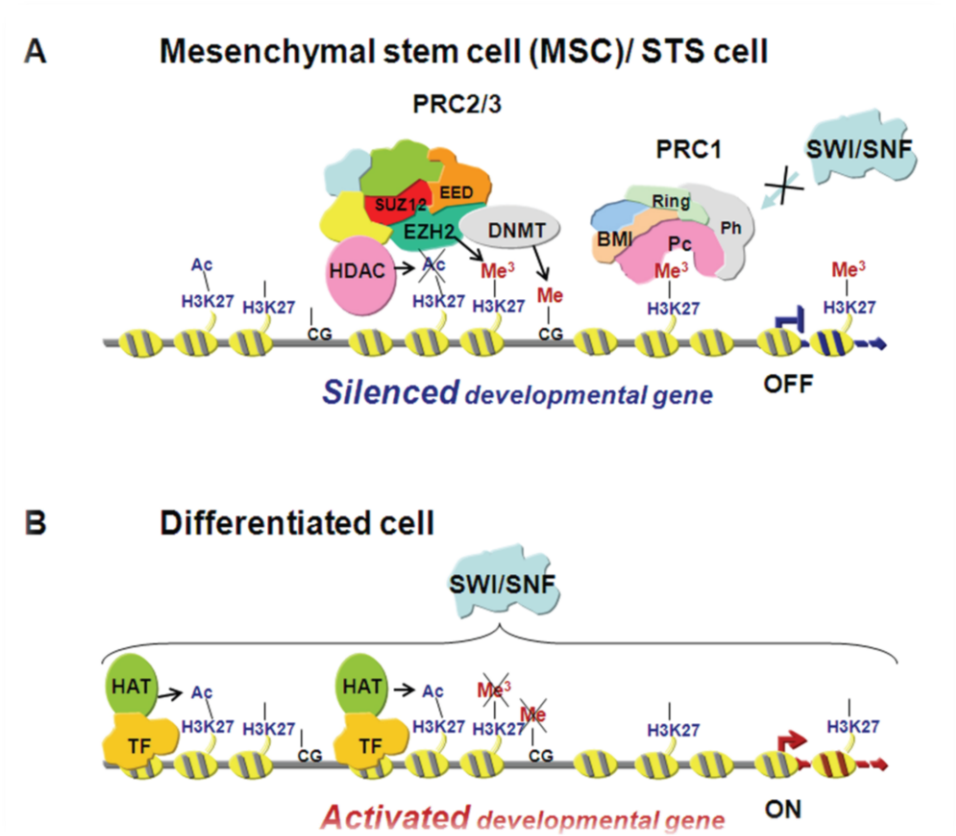

Figure 6. Schematic representation of transcriptional gene repression by EZH2. **(A)** EZH2 interacts with SUZ12 and EED in the initiation of gene repression. During differentiation **(B)** the expression of EZH2 decreases and H3K27 becomes hypomethylated and the SWI/SNF complex facilitates the binding of tissue specific transcription factors (TF) and histone acetyltransferase (HAT) to allow initiation of transcription [35].

PcG regulation is also well known to be involved not only in the maintenance of stem cell signature, but also in tumor development [33]. In mouse model; induced-overexpression of EZH2 in mammary epithelial cells may lead to epithelial hyperplasia [45]. Abnormal overexpression of EZH2 has been reported in a wide variety of tumor types including carcinomas, lymphomas, cutaneous melanoma, and soft tissue sarcomas [46]. Recent literature has been proved EZH2 is a useful auxiliary marker to discriminate between benign and malignant liver tumors [47]. High expression of EZH2

is generally associated with advanced stages of tumor progression, aggressive tumor behavior, and dismal clinical outcome [42]. Intriguing hypotheses have recently been formulated on the collaboration between EZH2 and SYT-SSX. Among which, SYT has been described to interact with transcription-enhancing trithorax group proteins such as the SWI/SNF chromatin remodeling complexes via its SNH domain, while SSX has been shown to bind with the transcription-silencing PcG proteins such as EZH2 via its SSXRD domain. SYT-SSX is hypothesized to bring together these oppositely acting protein complexes, allowing each to exert their function, causing genetic deregulation and contributing to sarcomagenesis [10, 22]. Interestingly; the binding of PRC1 hinders the access of other chromatin remodeling complexes such as SWI/SNF, that may have transcription-enhancing functions **(Figure 6)** [48], which implies, at least partly, that out of the antagonistic partners of SYT-SSX in synovial sarcoma, PcG may ultimately dominate over SWI/SNF [22, 35]. On the other hand, recent literature also indicates that SWI/SNF can also oppose the evict PcG [23, 24] implying the controversial underlying biochemical mechanisms. Identification of possible target genes influenced by this epigenetic deregulation has begun, but much effort is still needed to elucidate the pathomechanism in full detail [49].

I.5 Possible origin of tumor cells

Due to the uncertainty of its origin; synovial sarcoma is still among category of so-called "tumors of uncertain differentiation" in the latest edition of "World Health Organization Classification of Tumors" [2].

Research has found that synovial sarcoma cells possessed stem cell-like traits expressing stem cell-associated genes such as *Sox2, Oct4, Nanog,* they formed sarcospheres during cell culture and the abilities to differentiate into osteocytes and

chondrocytes [1]. After silencing the expression by small interrupting RNA, the sarcospheres become adherent monolayer; they also showed later mesenchymal lineage-specific genes (e.g. *Sox9, Runx-2* and *PPARγ*)and adipose tissue differentiation indicating synovial sarcoma may be a mesenchymal stem cell tumor [1]. Expression of *SYT-SSX* fusion gene in bone marrow-derived mesenchymal stem cells showed not only up-regulation of genes related to neuronal development but also disrupted its normal differentiation such as adipogenesis [1, 27, 32] implying the fusion protein may exert certain degree of pressure toward neuronal differentiation in mesenchymal stem cells and induces oncogenesis through stimulation of lineage commitment and simultaneous prevention of terminal differentiation.

In transgenic mouse model; tumor developed mimicking synovial sarcoma in myoblasts but not in more differentiated myocytes when transduced and expressed *SYT-SSX* fusion gene [50]. All these indicate that distinct cell populations at different developmental stages in the mesenchymal lineage hierarchy may serve as the cell of origin for synovial sarcomas.

The recent gene expression profiling study comparing human pluripotent stem cell and human mesenchymal stem cell induced by *SYT-SSX* revealed striking differences; the former showed mainly up-regulated genes and the later both up- and down-regulated genes could be observed and only less than half of the up-regulated genes were overlapping between these two groups indicating the cell context is important in synovial sarcoma tumor biology [51].

At the present moment, only mouse model showed weakly transforming activity of the fusion gene [16]; no fusion gene-based model of synovial sarcoma has been established so far using human mesenchymal stem cells [32, 52]. It is possible that mouse mesenchymal cells in culture are prone to have auto-transformation or the

microenvironment may also plays a role in vivo [52]. Since the fusion gene in soft tissue sarcomas mostly disrupts differentiation, the "2nd-hit" is expected to target the genes involved in proliferation and apoptosis checkpoints such as *p53* [53]. Hence, it is possible that the expression of *SYT-SSX* fusion genes in human mesenchymal stem cells per se is insufficient for synovial sarcoma initiation and secondary oncogenic hits will be needed to achieve the full transformation [52, 54]. This hypothesis is further supported by the overexpression of *MDM2, CDK4* and suppression of *INK4/ARF, Bim* are commonly found in synovial sarcomas [5, 27, 55].

I.6 Therapeutic strategy

Surgery remains the gold standard for synovial sarcoma management. Wide surgical excision with margins of 1 cm or more or margins involving fascia is crucial for local control of the tumor, for the tumors located at the extremity; limb-sparing procedures are preferred to amputation for the functional consideration. When the tumor is located in the large joints where wide excision is not achievable, adjunctive radiotherapy can be applied additional to local excision [56]. Synovial sarcoma is a relatively chemosensitive tumor. As to the other soft tissue tumors, only two chemotherapeutic agents, doxorubicin and ifosfamide showed complete or partial response [57-59].

Doxorubicin, the drug used in standard single agent chemotherapy protocols for the treatment results in only up to 25% response rates. Together with the ifosfamide, has not dramatically improved the overall 5-year survival rate higher than 50% [60]. Nevertheless, chemotherapy is still the choice for palliation for patients with metastases to improve the life qualities. Since the fusion protein-induced genetic deregulation plays a main role in synovial sarcoma. A charming aspect is the potential usage of target

DOI:10.14753/SE.2014.1917

therapy; with or without chemotherapy to maximize the treatment effect. This will be described more detail in the discussion session.

DOI:10.14753/SE.2014.1917

II. Objectives

Since synovial sarcomas are invariably high-grade tumors with 5-year overall survival rate varied between 36 to 76% depending on relatively poorly-defined criteria such as age, tumor size, mitoses, proportion of poorly differentiated areas and the resectability of tumors [5]. It has also been documented that aneuploidy DNA content is associated with adverse clinical course; however, it only explained partly since the majority (67%) of the cases was diploid which also plays a role in the prognostic variability [61]. In the other hand, regarding the karyotype, some research groups found tumors with complex karyotype had dismal clinical outcome whereas the others found no differences [55, 62].

Furthermore, although it is well documented that high EZH2 expression was shown to be generally associated with poor prognosis in soft tissue sarcomas [63], neither differential expression of EZH2 in the various histological subtypes of synovial sarcoma nor the association of EZH2 with H3K27me3, tumor behavior, and clinical parameters has been investigated in this particular tumor type in the recent literatures. Therefore, the goals of our project are as follow:

1. To investigate the DNA ploidy using image cytometry with fine-tune interpretation and correlates the result with high-resolution comparative genomic hybridization (HR-CGH) and clinical outcome.
2. To investigate the utility of EZH2 as a diagnostic marker in synovial sarcomas by comparing its expression (both in mRNA and protein levels) cross the histological subtypes, the molecular features and clinical data.
3. To elucidate the functional correlation between EZH2 and its epigenetic mark, H3K27me3.

4. To investigate the impact of EZH2 expression, along with H3K27me3 and Ki-67, on overall survival based on Kaplan-Meier curve.

III. Materials and Methods

III.1 Clinical data, tissue specimens and microarray

Fifty-five synovial sarcoma cases were selected for our study including 6 PDSS, 39 MPSS, and 10 BPSS fixed in 10% formalin and embedded in paraffin. From these, 9 cases fresh frozen samples containing 2 PDSS, 4 MPSS and 3 BPSS were also available for HR-CGH analysis. Tumor tissues were selected from the archives of the 1st Department of Pathology and Experimental Cancer Research, Semmelweis University, Budapest, Hungary, from the years between 1996 and 2009, and sampled by an expert soft tissue pathologist (Z.S.). Only primary tumors without preoperative chemo- or radiotherapy were chosen to avoid the post-therapeutic immunophenotypic changes. Clinical data (age, gender, tumor location, tumor size, presence or absence of metastases and the type of the fusion gene) were obtained from the institutional records. The numbers of male and female patients were 31 and 24, respectively. Age younger than 25 years was recorded in 8 cases, while 47 patients were older than 25 years. The mean age was 47 (range, 18-79). The tumor was located on the periphery in 39 cases and centrally in 16 cases. Tumors were larger than 5 cm in 14 cases. Distant metastasis was present in 31 cases. There were 35 cases associated with SYT-SSX1 fusion gene and 20 cases with SYT-SSX2 **(Table 2)**. All patients' information was coded, with complete clinical data available only for physicians involved in the treatment of these patients. The researches were conducted in concordance with the institutional ethical guidelines. Pathological diagnoses were made according to the World Health Organization (WHO) classification

[2], and confirmed by either FISH or RT-PCR for the fusion genes. Clinical follow-up data were also available for 32 cases (time after operation: 8-162 months). We used the same samples to construct tissue microarrays (TMAs) containing duplicates of 6-mm cores. In the specimens selected for HR-CGH analysis, the proportion of tumor cells were estimated after hematoxylin-eosin staining of tissue sections preceding to DNA extraction to assure in all cases the tumor cells comprised at least 85% of the total tissue areas.

III.2 Image cytometry

DNA smear for image cytometry was performed on 55 synovial sarcoma cases. From the formalin-fixed and paraffin-embedded (FFPE) samples, the nuclei were isolated before the smears were prepared. Three 50μm sections were cut from each paraffin block. The sections were deparaffinized in xylene and rehydrated in a series of decreasing concentration of ethanol. The tissue was digested in Carlsberg's solution (0, 1% Sigma protease XXIV; 0,1M Tris buffer; 0, 07M NaCl; pH 7, 2) for 45 min at 37°C in thermomixer. After filtration, the nuclear extract was washed in distilled water, the nuclei were fixed in 70% ethanol and dropped on glass slide to prepare a smear. We used DNA staining kit acc. (Merck, Darmstadt, Germany) for the Feulgen stain, consisting of applying HCl to the isolated nuclei for 10 minutes in a water bath and transferred into Schiff's reagent at room temperature for at least 50 minutes and then squashed in acetocarmine. DNA image data processing was carried out using a regular microscope with an image–sensing scanner connected to a regular personal computer with dedicated software installed (CYDOK R, Fa. Hilgers, Königswinter, Germany). 40x objective and an interference filter (565±10nm) were used. We used lymphocytes and granulocytes as reference cells. The tumor and reference cells were differentiated

based on their shape, size and the nuclear stain, respectively. At least 30 reference cells and 200 diagnostic tumor cells were analyzed on each smear. The integrated optical density (IOD) of Feulgen-stained reference cells was used as an internal standard for the normal diploid DNA content and it was also used to rescale into c-values. A diploid cell presents with a DNA amount of 2c, meaning two complements of each chromosome; a tetraploid cell contains four chromosomes of each number (4c), respectively. To define the aneuploidy we used the interpretations introduced by Haroske et al. [64]. The identification of DNA-aneuploidy can be confirmed by two fundamental procedures: stemline interpretation (SLI) and single cell interpretation (SCI). Ploidy grade (highest peak of DNA histogram) of the stemlines characterizes the method of SLI whereas cells with a DNA amount of more than 5c as limiting value (5c exceeding events) are recorded by SCI **(Figure 7)**. A DNA index (DI) is given for the stemlines based on the modal DNA amount of cell cycle during the G_1 phase [65].

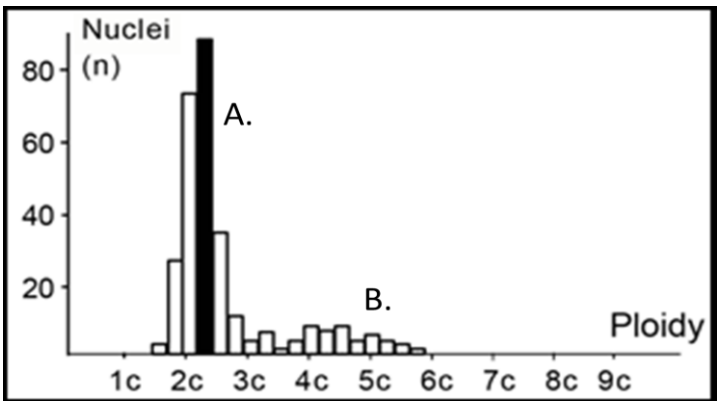

Figure 7. Illustration of histogram with stemline (A) and single cell (B) interpretations.

DNA aneuploidy is assumed when cells with a DNA content more than 2 times of G_1 phase of the reference cell fraction are detected. In tissues without polyploidization, 5c-exceeding events are sufficient for classification. The coefficient of variation of the reference cells was between 3% and 5%. Having measured the reference and tumor cells

separately; image analysis histograms were generated. DI of 1 corresponds to the 2c diploid DNA content. Between DI of 0.9 and 1.1 (range between 1.8 and 2.2 for c-value) the sample is considered to be diploid. Outside this range the tumor is regarded as aneuploid. For the diploid group, we further stratified as "Simple Diploid (Ds)" without 5c exceeding events and "Complex Diploid (Dc)" in which tumor had a diploid stemline but contained any cell among 5c exceeding events by SCI method.

III.3 Metaphase high-resolution comparative genomic hybridization

We had 9 cases of synovial sarcoma, with fresh frozen tissue samples, available for HR-CGH analysis. DNA was extracted with a standard salting out method according to Miller et al. [66]. Hybridization was performed based on the standard protocol [67]. Briefly, sex-matched normal and tumor DNAs were labeled with SpectrumRed-dUTP and SpectrumGreen-dUTP, respectively, by using nick translation kit (Vysis, Downers Grove, IL, USA). Hybridization was performed in a moist chamber at 37°C for 3 days in the presence of an access of unlabeled Human Cot-1 DNA (Vysis) to suppress repetitive DNA sequences. The metaphases were captured with epifluorescence microscope (Nikon Eclipse E600) equipped with a monochrome CCD camera, and were analyzed using LUCIA CGH-Advanced Statistics 1.5.0 software (Laboratory Imaging Ltd, Prague, Czech Republic). At least 15 karyotypes were analyzed in each case. Ratio profiles were evaluated by Dynamic Standard Reference Interval (DSRI) based on an average of CGH analyses using 16 normal DNAs instead of conventionally fixed thresholds. The gains and losses were detected by comparing the 99.5% confidence interval of the mean ratio profiles of the test samples with the 99.5% DSRI (**Figure 8**) [68].

DOI:10.14753/SE.2014.1917

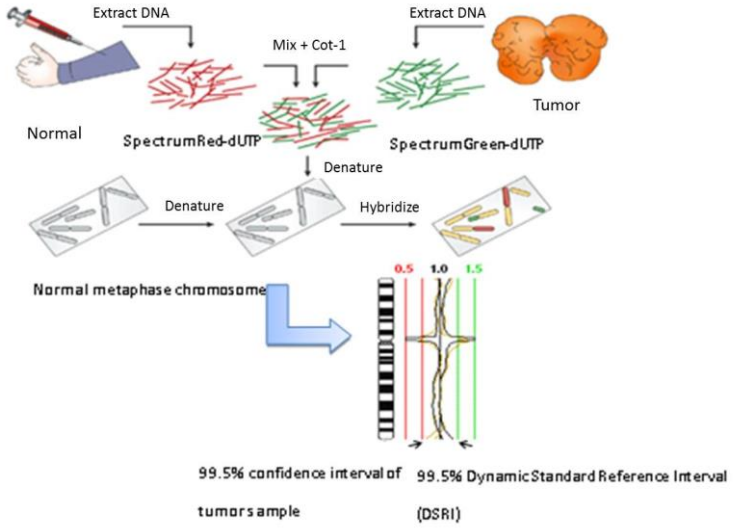

Figure 8. Illustration of HR-CGH (Modified from figure of HR-CGH note, Chromosome Laboratory, Copenhagen, Denmark)

Negative and positive controls were included in each experiment as well. Two differentially labeled DNAs (normal test and normal reference) hybridized together served as a negative control. Positive control was created from the specimens with a known trisomy 21, and partial deletion of chromosome 17, del(17)(p13). Heterochromatic regions in the centromeric and paracentromeric areas of the chromosomes, the short arm of the acrocentric chromosomes, and the Y heterochromatic as well as telomeric regions were excluded for the evaluation in order to decrease the background noise, and increase the diagnostic threshold as well as the accuracy.

III.4 Immunohistochemistry

After preparing 4-µm sections from the formalin-fixed, paraffin-embedded TMAs, sections were deparaffinized in xylene and rehydrated in a descending ethanol series. Antigen retrieval was achieved by using either Bond Epitope Retrieval Solution 1 (pH~6) or Bond Epitope Retrieval Solution 2 (pH~9) (Leica Microsystems, Wetzlar, Germany) at 99–100°C for 20–30 minutes. Monoclonal mouse anti-EZH2 (1:25, clone 11, BD Biosciences, USA), monoclonal rabbit anti-trimethyl-Histone H3 Lys27 (1:200, clone C36B11, Cell Signaling Technology, USA), and monoclonal mouse anti-Ki-67 (1:50, clone MIB-1; Dako, Denmark) antibodies were applied on the slides. Immunohistochemical staining was performed on a Leica BOND-MAX™ autostainer (Leica Microsystems, Berlin, Germany), and peroxidase/DAB Bond™ Polymer Refine Detection System (Leica Microsystems) was used for visualization.

III.5 Scoring criteria

To assess the immunohistochemical labeling of EZH2, H3K27me3, and Ki-67, immunostained slides were evaluated under a 10x magnification objective. "Nuclear staining intensity" was scored as follows: 0, no visible staining; 1, weak; 2, moderate; 3, strong. Higher score was chosen if at least 30% of positive tumor cells showed stronger intensity.

To quantify the "extent" of immunostaining, the percentage of tumor cells with positive nuclear reaction was counted, and a score was assigned as follows: 0, no visible staining; 1, 1–50%; 2, 51–75%; 3, over 75%. Each core contained at least 100 tumor cells to be evaluated. The two scores were summed to yield a final score ranging from 0 to 6. Fields of view representative of scores 0, 3, and 6 are shown in **Figure 9**. A total score ≤ 3 was defined as low and ≥ 4 as high.

DOI:10.14753/SE.2014.1917

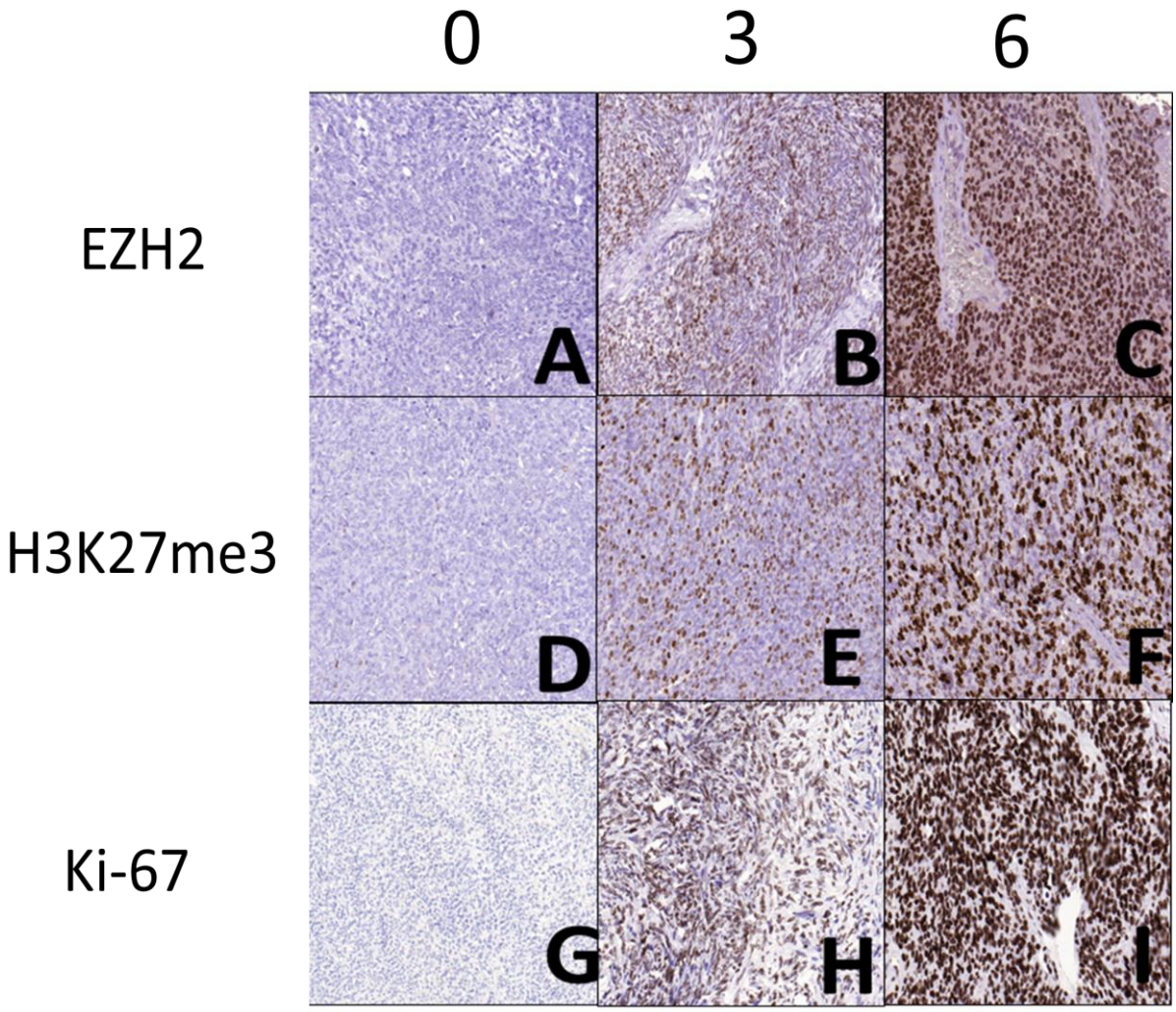

Figure 9. Photomicrographs representing the scores 0, 3, and 6 for EZH2 (A, B and C), H3K27me3 (D, E and F), and Ki-67 (G, H and I) immunostaning.

III.6 Analysis of EZH2 mRNA expression

For EZH2 gene expression analysis, total RNA was isolated from formalin-fixed, paraffin-embedded blocks of synovial sarcoma tissue by using RecoverAll™ Total Nucleic Acid Isolation Kit (Ambion, Austin, USA) based on manufacturer's instruction. Briefly; after deparaffinization, protease was added with digestion buffer and incubated in 70 ˚C for 30 minutes followed by nucleic acid isolation by adding isolation additive followed by sequence of centrifugation and washing procedure. DNase was added and

followed by washing procedure. The RNA was eluted by adding elution solution at room temperature. Due to the RNA degradation, the quality of isolated RNA was adequate for gene expression analysis in 13 MPSS, 2 BPSS and 6 BPSS cases. cDNA was generated from 1 µg of total RNA using High Capacity cDNA Reverse Transcription Kit (Applied Biosystems, Foster City, USA), following the instructions of the supplier. Quantitative real-time PCR (qRT-PCR) was performed in a LightCycler 480 Real-Time PCR System (Roche Applied Science, Indianapolis, USA) by using ABI TaqMan Gene Expression Assay for human *EZH2* gene (assay ID: Hs01016789_m1; Applied Biosystems) according to the manufacturer's protocol. The expression of *EZH2* was normalized to endogenous human ribosomal protein S18 (assay ID: Hs02387368_g1; Applied Biosystems), and cDNA from lymph node served as calibrator. Results were obtained as "crossing point (Cp)" values. Expression levels were calculated by using the $2^{-\Delta\Delta Cp}$ method.

DOI:10.14753/SE.2014.1917

III.7 Statistical analysis

Prism 4 software (GraphPad, USA), SigmaPlot and SigmaStat software packages (SPSS, version 11.0, IBM, USA) and the VassarStats website (www.vassarstats.net) were used for statistical analyses. Fisher's exact test was used to examine whether the aneuploidy, complex diploid and simple diploid groups, regarding the prognosis, were significantly different. On the other hand, in order to compare the immunohistochemical scores of EZH2, H3K27me3 and Ki-67, Kruskal-Wallis test was used for the comparison of more than two groups, while pairwise comparison of non-Gaussian data sets was done by the Mann-Whitney test. Correlations were analyzed by the Spearman's rank order correlation test (Spearman's rho, ρ) and coefficient of determination (R2). Kaplan-Meier curves were created based on the duration of survival after operation, and groups were compared with univariate analysis using the log-rank test. For all analyses, P values <0.05 were considered as statistically significant.

DOI:10.14753/SE.2014.1917

IV. Results

IV.1 Significant differences among aneuploid, simple diploid and complex diploid groups

The results of immunostaining and image cytometry are summarized in **Table 2.** From our 55 synovial sarcoma cases; 10 cases (17.9%) were aneuploid by image cytometry, and the mean DI was 1.40 **(Figure 10)**. Among those; all six cases of PDSS were found aneuploid.

DOI:10.14753/SE.2014.1917

Table 2. Clinical and image cytometry data, immunohistochemical scores, and EZH2 gene expression values of 55 synovial sarcoma cases.

Sample ID	Gender	Age	Size	Location	Subtype	SSX	DNA index	Histogram	EZH2 total score	H3 total score	Ki67 total score	metastasis	$2^{-\Delta\Delta Cp}$	Follow up (month)	End Point
1	M	30	0	P	biphasic	1	1,08	Dc	0	0	0	no	0,15	162	0
2	M	37	1	P	poorly differentiated	1	1,15	A	6	5	5	yes	2,53	12	1
3	F	35	1	P	poorly differentiated	2	1,21	A	6	6	6	yes	1,11	8	1
4	M	66	0	P	monophasic	2	0,96	Dc	2	2	0	no	0,18	NA	NA
5	F	60	0	P	monophasic	1	0,96	Dc	2	3	2	yes	0,36	NA	NA
6	M	35	0	P	monophasic	1	0,93	Ds	2	2	2	no	0,34	65	1
7	M	52	NA	P	monophasic	2	1,07	Ds	3	2	3	yes	0,35	60	0
8	M	79	0	P	biphasic	1	0,95	Ds	4	4	4	yes	NA	84	1
9	F	65	NA	C	monophasic	1	1	Ds	3	3	3	no	NA	NA	NA
10	M	52	0	P	poorly differentiated	2	1,64	A	5	6	5	yes	2,51	53	1
11	F	51	0	P	monophasic	2	0,95	Ds	0	0	0	no	1,11	132	0
12	M	43	NA	C	monophasic	1	0,91	Ds	2	3	0	no	NA	NA	NA
13	M	59	NA	C	monophasic	1	1,26	A	2	0	2	no	NA	NA	NA
14	M	52	1	P	monophasic	1	1,34	A	2	2	0	no	0	48	1
15	F	78	NA	P	monophasic	1	1,01	Ds	3	0	3	yes	NA	NA	NA
16	F	21	0	P	biphasic	1	1,06	Ds	2	2	3	yes	0	72	1
17	F	39	NA	P	monophasic	2	0,96	Ds	3	2	3	no	NA	NA	NA
18	F	39	NA	P	monophasic	2	0,92	Ds	3	3	3	no	NA	NA	NA
19	F	22	NA	C	biphasic	1	0,93	Ds	2	2	2	no	0	NA	NA
20	M	52	0	C	monophasic	1	0,97	Ds	3	2	2	yes	NA	NA	NA
21	F	54	NA	P	monophasic	1	1	Ds	2	2	2	yes	NA	NA	NA
22	M	46	1	P	monophasic	2	0,98	Ds	3	2	1	no	0,68	18	1
23	M	68	NA	P	monophasic	2	0,96	Ds	0	2	1	no	0	74	0
24	F	36	NA	P	monophasic	1	0,93	Ds	2	3	3	yes	NA	NA	NA
25	F	70	0	C	monophasic	1	1,05	Ds	2	2	2	yes	0,46	NA	NA
26	M	44	0	C	monophasic	1	1,04	A	2	2	2	yes	NA	36	0
27	M	52	0	P	monophasic	1	0,98	Ds	0	0	1	no	0,08	39	0
28	M	44	0	P	biphasic	1	1,19	Ds	2	2	1	no	NA	NA	NA
29	M	31	1	P	poorly differentiated	2	1,85	A	5	4	4	yes	0,56	22	1
30	F	74	0	C	monophasic	2	0,95	Ds	0	2	0	no	0	72	0
31	F	66	0	C	monophasic	2	0,94	Ds	2	2	3	no	NA	60	0
32	F	24	1	C	monophasic	2	0,9	Ds	2	2	0	yes	NA	36	0
33	M	18	0	P	monophasic	1	1,09	Ds	2	2	2	no	NA	55	0
34	M	18	0	P	monophasic	1	0,92	Ds	2	2	0	no	NA	46	0
35	M	27	1	P	monophasic	2	0,97	Ds	2	2	0	no	NA	72	0
36	F	64	0	C	monophasic	2	0,99	Ds	2	2	0	no	NA	75	0
37	F	29	NA	C	biphasic	1	0,99	Ds	2	2	2	no	NA	NA	NA
38	F	29	NA	P	biphasic	1	1	Dc	4	3	0	yes	NA	NA	NA
39	F	36	NA	P	biphasic	1	1,08	Dc	3	3	0	yes	NA	NA	NA
40	F	36	0	P	biphasic	1	1,07	Dc	2	2	0	yes	NA	61	1
41	M	44	NA	C	monophasic	1	1,04	Dc	2	3	2	yes	NA	NA	NA
42	M	29	1	P	poorly differentiated	1	1,17	A	6	6	5	yes	5,68	30	1
43	F	41	1	P	biphasic	1	1,03	Dc	4	4	4	no	NA	48	0
44	M	61	0	P	monophasic	1	0,95	Dc	3	4	3	no	NA	47	0
45	M	18	NA	P	monophasic	1	0,95	Ds	4	4	2	yes	NA	NA	NA
46	F	42	1	C	monophasic	2	1,02	Ds	4	3	2	yes	NA	33	0
47	M	19	NA	C	monophasic	1	0,95	Ds	3	3	3	no	NA	NA	NA
48	M	19	NA	P	monophasic	1	0,92	Ds	5	5	2	yes	NA	NA	NA
49	M	33	1	P	monophasic	2	1,03	Ds	4	2	3	no	NA	48	0
50	M	65	1	C	poorly differentiated	1	1,51	A	6	5	5	yes	2,12	15	1
51	M	65	0	P	monophasic	1	1,6	A	3	3	3	yes	NA	24	0
52	M	54	NA	P	monophasic	2	1,02	Ds	4	3	2	yes	NA	NA	NA
53	F	75	0	P	monophasic	1	0,95	Dc	3	2	3	yes	0,77	NA	NA
54	M	67	1	P	monophasic	2	0,94	Dc	4	2	2	no	NA	36	0
55	F	55	1	P	monophasic	2	1,03	Dc	3	2	3	no	NA	24	0

(gender: M: male; F: female; size: 0, <5cm; 1, ≥5cm; location: P, peripheral; C: central; end point: 1, deceased; 0, alive at the indicated time point (months post-operatively.);

A: aneuploid; Ds: simple diploid; Dc: complex diploid; NA: data not available.)

DOI:10.14753/SE.2014.1917

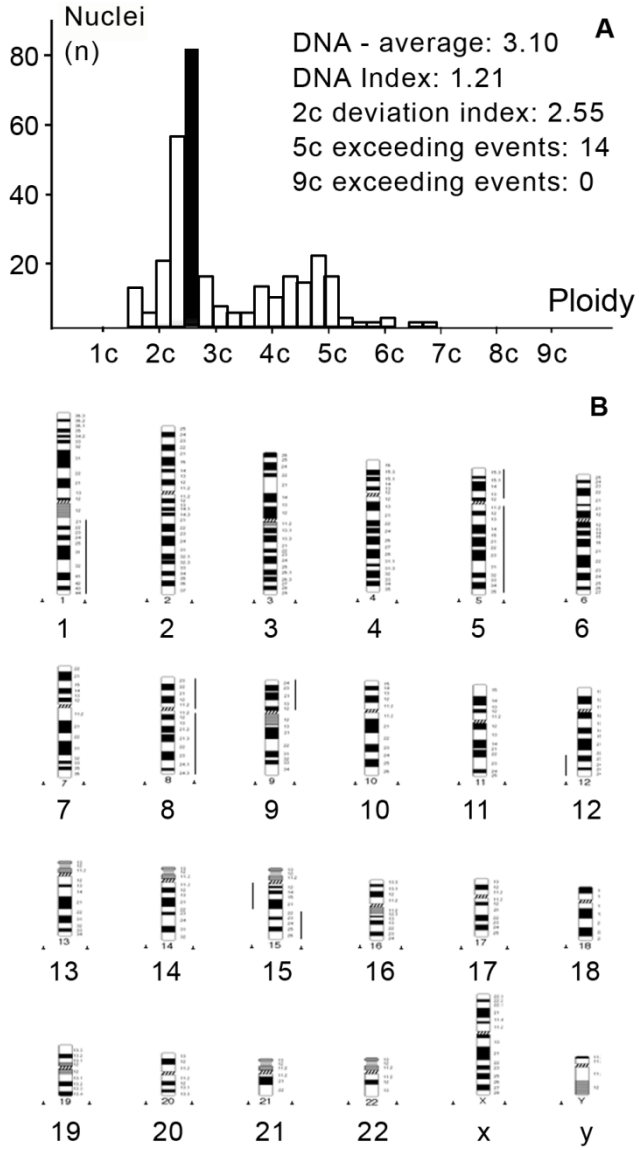

Figure 10. Representative DNA histogram **(A)** and HR-CGH ideogram **(B)** of aneuploid synovial sarcoma (case 2). Aneuploid tumor with a complex gain (1q, +5, +8, 9p, 12p13-q22, 15q22-26) and loss (12q23-24, 15q11.2-21) of DNA content. DNA index was found to be 1.21. The lines at the right of the chromosome ideogram represent DNA gains, lines at the left, DNA losses.

The histogram of the other 45 cases (82.1%) represented diploid tumor with 0.99 mean DI. Fine-tuned analysis was performed on this group according to the 5c exceeding events which represent single cell aneuploidy.

Thirty-three cases (71.7% of total diploid cases) without 5c exceeding events were considered as simple diploid **(Figure 11).**

DOI:10.14753/SE.2014.1917

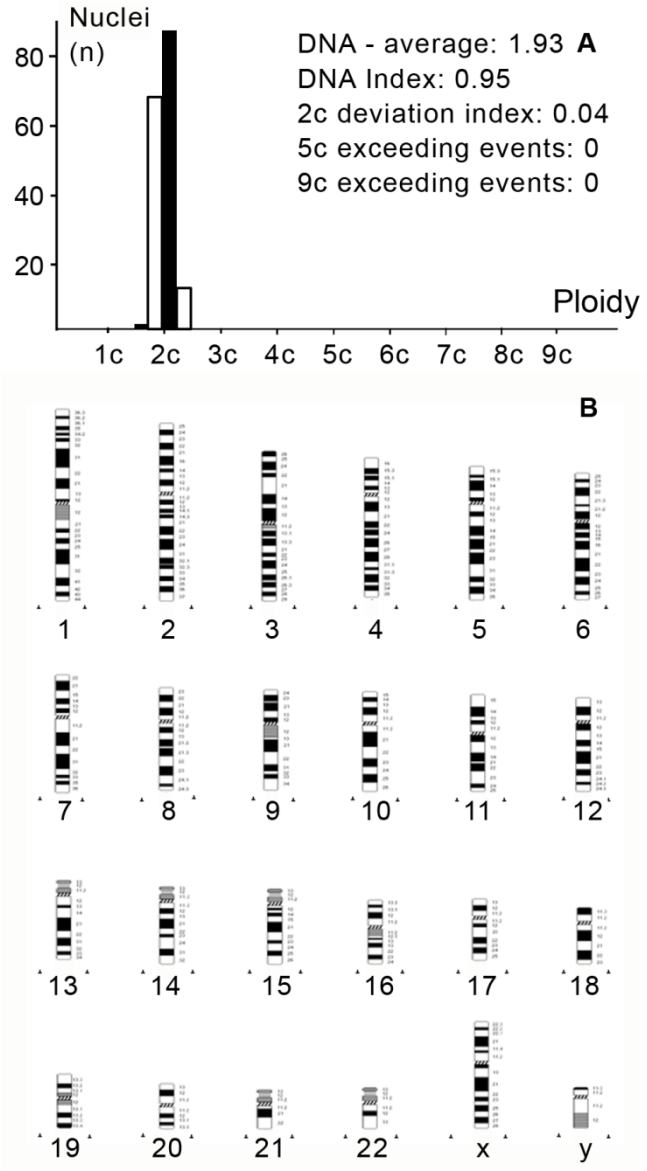

Figure 11. Representative DNA histogram **(A)** and HR-CGH ideogram **(B)** of a simple diploid synovial sarcoma (case 6). Note there is no cell above the 5c value and there is no alteration concerning the CGH results.

Twelve cases (28.3% of total diploid cases) fell into the complex diploid group containing 5c exceeding events any number **(Figure 12)**.

DOI:10.14753/SE.2014.1917

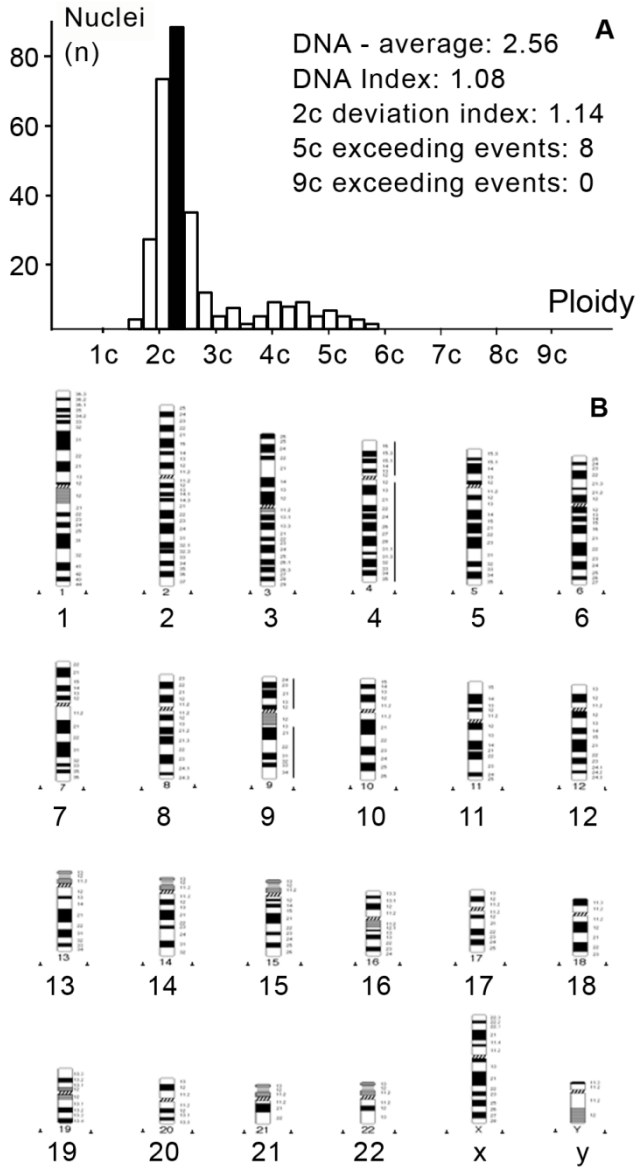

Figure 12. Representative DNA histogram **(A)** and HR-CGH ideogram **(B)** of a complex diploid synovial sarcoma (case 4). Though the tumor possesses diploid stemline; 8 cells proved to be above the 5c value. CGH revealed the gain of chromosomes 4 and 9.

It is important to know that only aberrations that are present in a high proportion among tumor cells can be detected by CGH. If the normal cell content is more than 50% of the tumor specimen, the evaluation may be difficult. Thus, the evaluation and selection of representative tumor material are crucial for the appropriate evaluation of CGH. The average tumor cell concentration in our cases was at least 85% (range from

85% to 100%).

HR-CGH analysis revealed chromosome imbalances in 5 out of the 9 (55.5%, 2 and 3 cases with aneuploidy and complex diploid DNA content, respectively) cases; in the other 4 cases, which showed simple diploid DNA content, neither chromosomal gains nor losses were found. The chromosomal imbalances found are listed in **Table 3**. The aneuploid tumors contained a large number of genetic alterations with the sum gain of at least 2 chromosomes within group A (chromosomes 1 to 3), B (chromosomes 4 and 5) or C (chromosomes 6 to 12) based on the length and centromere position. The single alterations consisted of gains of chromosome 1p, 1q, 2q24-q37, 5, 7q11.2-q36, 8, 8q23-24, 9p, 12p13-q22 and 15q22-26 and losses of chromosome were 3p14-p26, 4, 5p14, 12q23-24, 13q12-q22, 15q11.2-21, 16q and 18q12-q22 **(Figure 10)**. The complex diploid samples showed less but substantial aberrations (at least 3) such as gains of chromosome 3q, 4 and 9, and losses of chromosome 1p12-22, 3p, 4q28-q35, 5q15-35, 6q12-q23, 16q, 19, 20 and 22 **(Figure 12)**. In simple-diploid cases no genetic alterations could be detected by HR-CGH **(Figure 11)**.

Table 3. High-resolution comparative genomic hybridization data of 9 synovial sarcoma cases

No.	Ploidy	Chromosome Gains	Chromosome Losses
1	A(PDSS)	1p, 2q24-q37, 7q11.2-q36, +8, 8q23-24	3p14-p26, -4, 5p14, 13q12-q22, 16q, 18q12-q22
2	A(PDSS)	1q, +5, +8, 9p, 12p13-q22, 15q22-26	12q23-24, 15q11.2-21
3	Dc(MPSS)	+4, +9	none
4	Dc(MPSS)	3q	1p12-22, 3p, 5q15-35, -19, -20, -22
5	Dc(BPSS)	none	4q28-q35, 6q12-q23, 16q
6	Ds(BPSS)	none	none
7	Ds(BPSS)	none	none
8	Ds(MPSS)	none	none
9	Ds(MPSS)	none	none

(A, aneuploid; Dc, diploid-complex; Ds, diploid-simple)

Concerning the clinical course, 8 out of 10 patients (80%) with aneuploid tumor, 13 out of 33 patients (39%) with “simple-diploid” tumor and 6 out of 12 patients (50%) with “complex-diploid” tumor developed metastasis, respectively. By using Fisher’s exact test the three groups proved to be significantly different (P = 0.04).

IV.2 High expression of EZH2 and high abundance of H3K27me3 in PDSS

Concerning the EZH2 expression in synovial sarcomas; percent distribution of immunohistochemical scores is illustrated in **Figure 13A**, and statistical results are summarized in **Table 4**. Similar to Ki-67, high immunohistochemical scores of EZH2 and H3K27me3 were specifically recorded in PDSS and only rarely in the other subtypes. Overexpression of EZH2 in PDSS relative to MPSS and BPSS was also confirmed at the mRNA level (8.1x higher expression in PDSS, P<0.001, **Figure 13B)**. Significant differences between PDSS, MPSS and BPSS for EZH2, H3K27me3 and Ki-67 immunohistochemical scores were detected by Kruskal-Wallis test (all P<0.001). The mean scores of all three markers were significantly higher in PDSS as compared with MPSS and BPSS. Furthermore, scores of EZH2 and H3K27me3, but not of Ki-67, were significantly higher in patients with larger tumor size, and all three markers were significantly higher in those with distant metastasis **(Table 4)**. No statistically significant differences in mean immunohistochemical scores were found with regard to clinical factors such as age, gender, tumor location, or the type of fusion gene. Thus, EZH2 and H3K27me3 may be regarded as auxiliary markers of the poorly differentiated subtype, although the potential of EZH2 and H3K27me3 immunostaining to discriminate between PDSS and the other subtypes was inferior to that of Ki-67 (sensitivities, specificities, and positive predictive values for EZH2: 1.00, 0.82, 0.4; H3K27me3: 1.00, 0.90, 0.54; Ki-67, 1.00, 0.96, 0.75, respectively).

DOI:10.14753/SE.2014.1917

Across all subtypes, EZH2 expression was found to correlate with the abundance of H3K27me3 mark **(Figure 14A, ρ: 0.73, P<0.0001, R^2=0.648)**, indicating causal relationship between EZH2 activity and the presence of the associated epigenetic mark in synovial sarcoma. Significant positive correlation could also be demonstrated between EZH2 and Ki-67 scores both when including all cases **(Figure 14B, ρ: 0.65, P<0.0001, R^2=0.519)** and with the exclusion of PDSS cases **(Figure 14C, ρ: 0.50, P<0.001, R^2=0.242)**, suggesting that EZH2 expression and proliferative activity were positively linked in the better-differentiated subtypes as well.

DOI:10.14753/SE.2014.1917

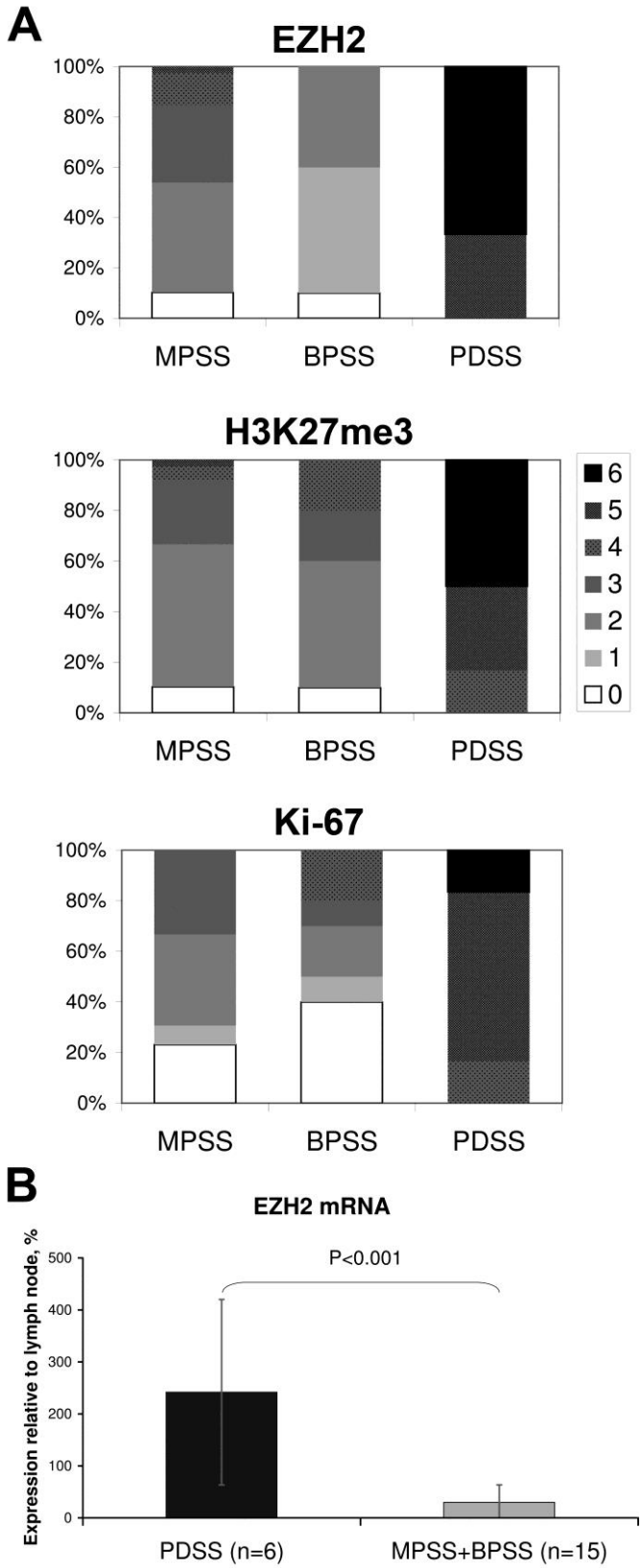

Figure 13. Distribution of scores 0–6 in the MPSS, BPSS, and PDSS subtypes, shown as stacked columns **(A).** mRNA expression of EZH2 in the PDSS vs. MPSS+BPSS groups, mean ± S.D. Human ribosomal protein S18 was used as endogenous control and human lymph node was served as calibrator **(B).**

DOI:10.14753/SE.2014.1917

Table 4. Comparison of immunohistochemical scores across patient groups sorted by histological subtype and clinical / molecular characteristics

Compared groups	*Statistical test used*	*Result*
EZH2		
PDSS and MPSS and BPSS	Kruskal-Wallis	P < 0.001
PDSS vs. MPSS	Mann-Whitney	P < 0.001
PDSS vs. BPSS	Mann-Whitney	P = 0.001
MPSS vs. BPSS	Mann-Whitney	NS
H3K27me3		
PDSS and MPSS and BPSS	Kruskal-Wallis	P < 0.001
PDSS vs. MPSS	Mann-Whitney	P < 0,001
PDSS vs. BPSS	Mann-Whitney	P = 0.001
MPSS vs. BPSS	Mann-Whitney	NS
Ki-67		
PDSS and MPSS and BPSS	Kruskal-Wallis	P < 0.001
PDSS vs. MPSS	Mann-Whitney	P < 0,001
PDSS vs. BPSS	Mann-Whitney	P = 0.001
MPSS vs. BPSS	Mann-Whitney	NS

Compared groups	*EZH2*	*Ki-67*	*H3K27me3*
Gender			
Male vs. female	NS	NS	NS
Age			
≤25 y/o vs. >25 y/o	NS	NS	NS
Location			
Central vs. peripheral	NS	NS	NS
Tumor size			
<5cm vs. ≥5cm	P < 0.001	NS	P = 0.032
Distant metastasis			
Present vs. absent	P < 0.001	P = 0.021	P = 0.003
Fusion gene			
SYT-SSX1 vs. SYT-SSX2	NS	NS	NS

(PDSS: poorly differentiated synovial sarcoma; MPSS: monophasic synovial sarcoma; BPSS: biphasic synovial sarcoma; NS: not significant)

DOI:10.14753/SE.2014.1917

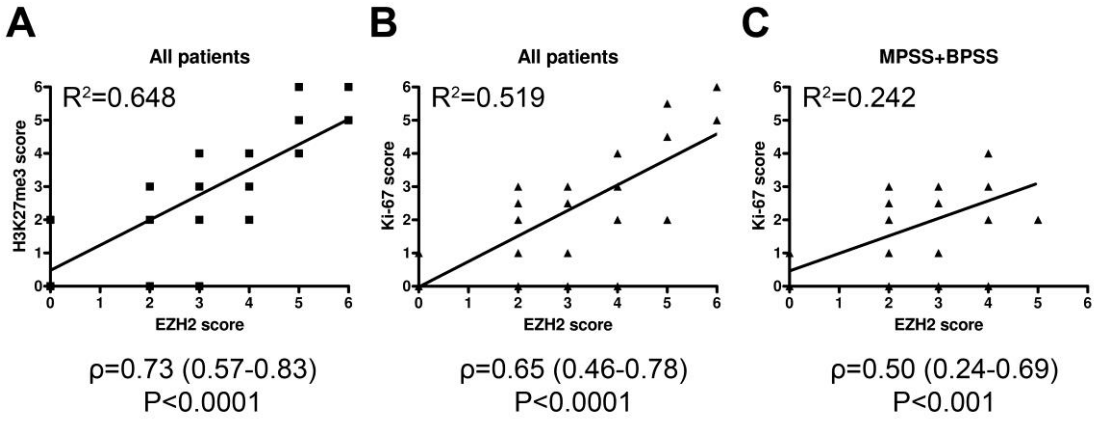

Figure 14. Scatter graphs with linear trend lines indicate positive correlations between EZH2 and the other markers**.** All patients were included in **(A)** and **(B),** while PDSS patients were excluded in **(C)**. Spearman's *r* (ρ) with 95% confidence intervals and coefficient of determination (R^2) values are also shown.

IV.3 EZH2 as a potential prognostic marker in synovial sarcoma

Kaplan-Meier curves generated by separating patients on the basis of high versus low EZH2 and H3K27me3 scores were similar to the one based on Ki-67 score **(Figure 15)**. However, Ki-67 was a superior predictor of tumor-associated death, since the hazard ratios referring to high EZH2, H3K27me3, and Ki-67 expression were 4.48, 5.65, and 6.32, respectively. Nevertheless, high EZH2 score also proved to be a valuable predictor of disease outcome, since it was significantly associated with larger tumor size, implying faster tumor growth, and the presence of distant metastasis. Moreover, these associations held true not only in the entire patient population but also after the exclusion of PDSS cases. In contrast, high H3K27me3 failed to show such associations, and high Ki-67 was associated with larger tumor size in all patients only **(Table 5)** indicating that EZH2 may be useful in the stratification of MPSS and BPSS patients into low and high risk prognostic groups with respect to the likelihood of developing distant metastasis.

DOI:10.14753/SE.2014.1917

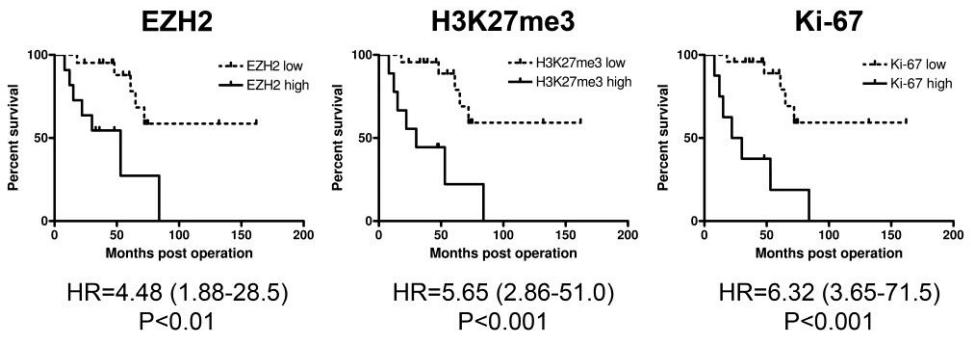

Figure 15. Kaplan-Meier survival curves for high vs. low EZH2, HeK27me3, and Ki-67 score. Hazard ratios (HR) of the high-score groups with 95% confidence intervals are shown at the bottom.

Table 5. Association of high EZH2, H3K27me3, and Ki-67 scores with the risk of tumor size and metastasis

	Relative Risk	95% Confidence Interval	P value
High EZH2 score			
All Cases			
-Tumor size >5 cm	4.09	1.78-9.40	P<0.001
-Distant metastasis	2.20	1.49-3.23	P<0.001
Cases other than PDSS			
-Tumor size >5 cm	4.00	1.63-9.82	P=0.02
-Distant metastasis	2.09	1.36-3.21	P=0.02
High H3K27me3 score			
All Cases			
-Tumor size >5 cm	2.25	1.07-4.73	NS
-Distant metastasis	1.64	1.09-2.46	NS
Cases other than PDSS			
-Tumor size >5 cm	1.12	0.20-6.17	NS
-Distant metastasis	1.20	0.55-2.60	NS
High Ki-67 score			
All Cases			
-Tumor size >5 cm	2.62	1.29-5.34	P=0.04
-Distant metastasis	1.71	1.17-2.51	NS
Cases other than PDSS			
-Tumor size >5 cm	1.75	0.39-7.88	NS
-Distant metastasis	0.98	0.24-4.03	NS

(NS: non-significant)

DOI:10.14753/SE.2014.1917

V. Discussion

It has been decades since the synovial sarcoma-specific translocation gene SYT-SSX has been discovered. Little is known regarding its role and its downstream signaling pathway contributing to the sarcomagenesis. Therefore, optimal therapeutic strategy and prognostic prediction are difficult to achieve at the present moment. It is possible that the specific translocation is essential for the initiation of tumorgenesis, however, during tumor progression (e.g. recurrence or metastasis), beside the anaplastic morphological changes, further genetic alterations also play crucial roles. Since these genetic alterations arise randomly (typical losses and gains of chromosomes or chromosomal segments are not known) [55, 62], measurement of the total DNA content gains high importance in estimating the prognosis of the disease and accordingly [61], in terms of the selection of the aggressiveness of the therapy. Majority of synovial sarcomas, irrespective of the histological subtype, exhibit simple karyotypes additional to its specific t(X;18) translocation. Secondary genetic anomalies are sometimes seen, but these alterations are often variable and inconsistent, and they are most frequently seen in recurrent or metastatic lesions. A recent case report of BPSS with genomic instability showed great cytogenetic heterogeneity in chromosome numbers and the recurrent presence of dicentric chromosomes which, in turn, may cause chromosome number abnormality in the subsequent mitoses [69]. Nevertheless, how the biological behavior of the tumor is affected by cytogenetic changes still needs to be uncovered.

The prognosis of synovial sarcomas varies; some develop metastases long (5-10 years) after the initial diagnosis while others are more aggressive. This can only be partly explained by “well-known” prognostic factors such as patient’s age, tumor size, extent of poorly differentiated areas and the resectability of tumor. Although karyotyping and CGH analyses provide excellent insights into the genetic alterations

of tumors, they are considerably time consuming and they are expensive methods. Measurement of the total DNA content by image cytometry can be not only a faster tool but also easier and cheaper to perform. Thus, the aim of the first part of our work was to detect whether the more frequently occurring diploid synovial sarcomas could be further divided into subgroups and the correlation with karyotype complexity. Although CGH is a powerful method for detecting DNA copy number changes of the entire genome, it only detects "gross" genetic abnormalities of the tumor specimen. Furthermore, only aberrations involving losses or gains of DNA sequences (unbalanced chromosomal aberrations) can be detected, whereas balanced chromosome abnormalities, such as reciprocal translocations, inversions, and point mutations are not detectable since they do not change the copy number [67]. CGH also cannot recognize the changes if the fraction of normal cells is high or if cells are polyploid. Therefore, normal findings may be false negative. The samples in our HR-CGH contained high fraction (range from 85 to 95%, estimated visually under hematoxylin eosin stain) of tumor cells to avoid the previously mentioned biases. Our results showed a correlation between DNA ploidy and the HR-CGH results. Complex diploid cases showed numerous genetic alterations whereas the simple diploid group, chromosome aberrations were hardly detectable. Among our HR-CGH results, we found the most frequent chromosome alterations, compared to the literature, are: gain of chromosome 2, 8, 12p, 12q and loss of 3p [55, 62]. The most likely candidate genes at 12q13-12q15 are *MDM2, CDK2, ERBB3, SAS* and *CDK4*; and *RASSF1*, a tumor suppressor gene located at 3p21.3. A clear association was described between gain of *SAS*, found in our aneuploid case, a member of the transmembrane 4 superfamily mediating cell development, activation, growth and motility, and its overexpression may lead to poor prognosis [55] whereas *MDM2*, *CDK2* and *CDK4* are involved in cell cycle regulations, once they get abnormally overexpressed, may result in abnormal

proliferation and transformation. It is important that the complex diploid tumors should not be regarded as aneuploid, even the complex karyotype is revealed by CGH analysis. It may be explained as individual cells with 5c exceeding events (single cell aneuploidy) within the diploid background (by stemline interpretation) which, in turn, contribute to the complex karyotype. Single cell aneuploidy is a well-known phenomenon and its detection is applied e.g. in the diagnostics of cervical dysplasia/carcinoma and ovarian borderline tumors/carcinomas as well [61, 70]. Although these 3 groups (simple diploid, complex diploid and aneuploid) were statistically different, we cannot be completely certain about the unequivocally good prognosis of the simple diploid cases since 39% within this group still developed metastasis. However, the tendency is unambiguous; by detecting single cell aneuploidy in the diploid group, we know that it means a complex karyotype at cytogenetic level and which certainly should not be regarded as usual diploid population. Therefore, there is a simple, inexpensive and fast tool available to provide important complementary data which may be beneficial for the further management.

In the second part of our work; high expression of EZH2 was predominantly found in the poorly differentiated histological subtype of synovial sarcoma, which was associated with aggressive clinical behavior. High levels of EZH2 were shown to be associated with poor clinical outcome in other tumor types as well, and the mechanisms that link EZH2 activity with tumor progression are gradually being unfolded [42].

V.1 Possible mechanisms of EZH2 overexpression

The exact causes and consequences of EZH2 overexpression in PDSS remain to be clarified. Nevertheless; several possibilities can be addressed:

V.1.1 MYC is upregulated in PDSS

Firstly, with regard to its transcriptional regulation, a hypothetic role can be assigned to *MYC* gene, since recent gene expression profiling data in PDSS revealed up-regulation of genes located on chromosome 8q, including *MYC*, and also down-regulation of the genes involving in cell-cell adhesion (e.g. *E-cadherin)*, neuronal and myogenic differentiation [71] which reflect the suppression of differentiation and high incidence of metastases. In prostatic carcinoma, *MYC* has been reported to induce EZH2 overexpression by 2 distinct mechanisms; it can bind to the promoter region of EZH2 and up-regulates its expression. It can also down–regulate miR-26a by binding to the parental promoter, *Pol II* and miR-26a, in turn, can repress EZH2 expression [72]. Interestingly, in rhabdomyosarcoma; the lack of mature skeletal muscle differentiation is also attributed by lack of miR-26a [73] implying deregulation of EZH2 and miR-26a is a common pathway for different tumor formations.

V.1.2 Hypoxia induced HIF1α up-regulates EZH2

Secondly, in breast carcinoma, EZH2 expression may also be triggered by hypoxia, a condition present in nearly all solid tumors. Hypoxia induced-HIF1α binds to the promoter region and up-regulates EZH2 which in turn repressed DNA damage repair gene such as *RAD51* and consequently causing chromosomal instability and amplification of *RAF1*. The overexpressed *RAF1* may activate ERK/β-catenin signaling pathway can lead to proliferation and expansion of mammary tumor-initiating cells [74].

V.1.3 Translocation-associated fusion proteins up-regulate EZH2

Further, EZH2 can also be induced by chimeric fusion protein. In Ewing sarcoma, EZH2 is up-regulated by direct binding of EWS-FLI1 fusion protein to its promoter region and down-regulation of EZH2 by siRNA suppressed the oncogenic transformation by inhibiting clonogenicity in vitro and reactivated neuroectodermal differentiating gene such as *EMP1* suggesting the role of EZH2 in tumor formation in keeping their primitive mesenchymal signatures [75].

V.1.4 microRNA associates EZH2 overexpression

At the post-transcriptional level, microRNAs are likely to modulate EZH2 levels, since EZH2 is a validated target of the promyogenic miR-26a, which normally, in myoblasts, binds to the 3' untranslated region (UTR) and undergoes degradation. In rhabdomyosarcoma high expression of EZH2 was consistently paralleled by down regulated miR-26a, and it binds to the PcG-associated transcription factor YY1 and further suppressed another promyogenic microRNA, miR-29, which is a negative regulator of YY1. The net result is EZH2 up-regulation and augmenting the function of PcG [73]. Another microRNA, miR-101, which also targets the EZH2 mRNA and promotes its degradation is also frequently lost in metastatic prostate carcinomas [76]

V.2 Genetic deregulation by EZH2

Although the target genes of EZH2-mediated silencing in synovial sarcoma still wait to be identified, EZH2 activity is generally thought to favor the conservation of undifferentiated state and give way to rapid proliferation. Significantly overlapping of mesenchymal stem cell-associated genes such as *Sox2*, *Oct4* and *Nanog*; and a subset of PRC2 target genes were found between metastatic prostatic carcinoma and embryonic cells, and the repression of these genes was associated with poor clinical outcome [77].

EZH2 is therefore believed to drive tumor cells into a more aggressive, embryonic stem-like state, as it is clearly exemplified by EZH2-overexpressing tumors with embryonic morphology like rhabdomyosarcoma, Ewing's sarcoma [35], and also in our study, synovial sarcoma. EZH2 can facilitate cell cycle progression: its expression is induced by E2F, a chief coordinator of mitotic entry, while EZH2 itself represses, among others, the tumor suppressor INK4/ARF and the pro-apoptotic regulator Bim [46, 78, 79]; all these mechanisms drive the cells in to the proliferative state. Our findings indicate that the link among EZH2 expression, high mitotic activity, and undifferentiated morphology exists in synovial sarcoma as well, since EZH2 scores strongly correlated with those of Ki-67 and were highest in PDSS. EZH2 may repress the expression of E-cadherin, which leads to epithelial-mesenchymal transition [80], and VEGF can transactivate EZH2 through E2F up-regulation; subsequent overexpressed EZH2, in turn, silences Vasohibin1, the negative regulator of angiogenesis, and augments the angiogenesis [81]. These all contribute to tumor aggressiveness and potential metastasis. On the other hand; the opposite can also be true since the recent research data also shows in appropriate context, expression of the SYT-SSX oncogene may destabilize the PRC1 subunit, Bmi1, resulting in impairment of PcG associated histone H2A ubiquitination and reactivation of the repressed target genes [82] indicating the activator/depressor role of the SYT-SSX in contributing sarcomagenesis is multifactorial and any imbalance in PcG activity could drive the cell toward oncogenesis.

V.3 EZH2 overexpression not always associates with H3K27me3

Another positive correlation found in our study, namely the one between EZH2 expression and the abundance of H3K27me3 marks, could be logically expected from the catalytic activity EZH2 is known to exert in PRC2. It is very interesting that, in many lymphomas (7% of follicular lymphoma and 22% of diffuse large B-cell lymphoma, respectively), the mutation of EZH2 was thought to inactivate the enzymatic activity of PRC2 [83], however, it was observed that wild-type EZH2 displays highest catalytic activity for the mono-methylation of H3K27, but weak for the subsequent di- and tri-methylation. On the other hand; in lymphoma, the Y641 mutant displays weak ability for catalyzing the mono-methylation, but acquires higher catalytic efficiency for the subsequent reactions. Additionally, the mutant Y641 allele in B-cell lymphomas is often heterozygous indicating the mutual complement effect and further augment H3K27 methylation, which may be functionally equivalent to EZH2 overexpression [42] and eventually leads to high H3K27 trimethylation [84, 85]. In contrary, nonsense mutation with stop codon before the SET domain is mostly found in myeloid tumors with hypomethylated histones [42], implying both activating and inactivating mutation of EZH2 may contribute to tumor, therefore, EZH2 may also be regarded as both proto-oncogene and tumor suppression gene simultaneously.

Additional to lymphomas, high levels of H3K27me3, as the consequence of EZH2 hyperactivity, have also been reported in hepatocellular carcinoma and esophageal squamous cell carcinoma [86, 87]. It is all the more intriguing why in certain tumors, such as carcinomas of the breast, ovary, and pancreas, no clear correlation between EZH2 expression and H3K27 trimethylation was found; rather, quite counterintuitively, both high EZH2 and low H3K27me3 turned out to have adverse prognostic significance [88]. Explanations proposed for this apparent discrepancy may be as follow:

V.3.1 Formation of Tumor-specific PRC

Since EZH2 on its own lacks enzymatic activity; this is conferred when it interacts with other subunits of PRC2 such as SZU12 and EED. In breast carcinoma, the EZH2 is overexpressed and the increased histone methyltransferase activity is achieved by coupling with these subunits or their isoforms. Therefore, abundance of EZH2 molecules may disrupt the integrity of the PRC complexes or induce the formation of other repressor complexes and, by altering the balance between different members among the PcG complexes, lead to the formation of tumor-specific PRC complexes that show different histone substrate specificities. It is documented that the newly formed PRC containing EED isoform 2 possesses substrate specificity to H1K26 instead of H3K17 [89]. As the result of decreasing H3K27me3, not only the general level of repression but also the specificity of repressed genes is changed [89] hence exacerbates the epigenetic deregulations. It is worth to mention that, additional to tumor-specific PRC, SYT-SSX fusion protein may also form tumor-specific SWI/SNF in the 5′-SYT (N-terminal) side which may evict SMARCB1 protein, remove H3K27me3 and reactive *Sox2* gene and increase proliferation [23] emphasizing the role as activator/depressor of SYT-SSX fusion protein

V.3.2 Akt-mediated inhibitory phosphorylation

The phosphoinositide 3-kinase–Akt (PI3K-Akt) signaling pathway is involved in processes such as survival, proliferation, growth and motility. It has been documented that Akt phosphorylates EZH2 at serine 21 and suppresses its methyltransferase activity by impeding the affinity of EZH2 binding to histone H3, possibly due to conformation changes, without altering the localization or the interaction with SUZ12 and EED, which results in a decrease of H3K27me3. Furthermore, knocking down Akt expression by siRNA may restore H3K27me3. Since H3K27me3 serves as an epigenetic mark

mediating silencing and represses target gene expression, loss of H3K27me3 expression may result in “de-repression” of these silenced genes, such as certain oncogenes, hence, contributing to tumor progression. The phosphorylated EZH2 may target non-histone substrates that are also an important factor for tumorigenicity. Hence, the changes of EZH2 substrate affinity mediated by Akt may also provide a possible explanation for the mechanisms underlying the loss of H3K27me3 [88, 90, 91].

V.3.3 Cyclin-dependent kinase associated regulation

Recent discoveries indicate that EZH2 is regulated by cell-cycle-dependent signaling through phosphorylation at Thr487 by CDK1 [92, 93] and it was shown that CDK1 phosphorylates EZH2 at Thr487 leads to disruption of the interaction among EZH2 and other PRC2 components. Phosphorylation of EZH2 at Thr487 [93], in another hand, also shows enhanced EZH2 ubiquitination and subsequent degradation [94]. The final consequence of the both mechanisms is reduced the methyltransferase activity and decreased H3K27me3.

By examining associations between EZH2 expression, histological subtype, and clinical factors such as tumor characteristics and disease course, we wished to clarify whether EZH2 (and/or H3K27me3) immunohistochemistry may provide any additional diagnostic, prognostic, or therapeutic information that cannot be deduced from other data. The markers investigated herein showed significant association with histology and distant metastasis, but varied independently from other clinical factors and the type of fusion gene. EZH2 and H3K27me3 scores also exhibited significant association with tumor size which may reflect the growth rate. Although Ki-67 distinguished more accurately between PDSS and the better-differentiated subtypes, both high EZH2 and high H3K27me3 were preferentially associated with PDSS. Further, whereas Ki-67 as a well-established prognostic marker in soft tissue sarcomas proved to be a superior

predictor of overall survival [95], high EZH2 status, but not high H3K27me3 or high Ki-67, was found to be predictive of fast tumor growth and distant metastasis in the MPSS+BPSS group may further explain the variable clinical outcome even in the better differentiated synovial sarcomas. Thus, while not sufficiently specific when applied alone, both EZH2 and H3K27me3 can be used as auxiliary immunohistochemical markers of the poorly differentiated subtype in doubtful cases (e.g., better-differentiated histomorphology coupled with high mitotic rate, or vice versa). Moreover, EZH2 status, along with other our previously finding, the prognostic impact of ploidy [96], may refine the current stratification of MPSS and BPSS patients into low- and high-risk subgroups, thus influencing prognosis and possibly also the therapeutic strategies.

Lastly, several molecular target therapies have been initiated for treating synovial sarcomas including anti-BCL-2 and anti-EGFR alone or combine with traditional chemotherapy regimens [97, 98]. G3139, an 18-base phosphorothioated antisense oligonucleotide complementary to the first six codons of the open reading from BCL-2 mRNA, designed to decrease BCL-2 expression and therefore allow apoptosis of cancer cells [99]. In vitro study showed augmented dose-dependent death of synovial sarcoma cells and increased apoptosis when used together with doxorubicin [56]. Additionally, although SYT-SSX increases BCL-2 expression, it has been documented it also represses other anti-apoptotic genes such as MCL-1 and BCL-2A1, the alternative anti-apoptotic pathways, which make synovial sarcoma sensitive to BH3-domain peptiomimtic (ABT-263) therapy [100]. Pazopanib, a multi-kinase inhibitor also revealed inhibiting the growth of synovial sarcoma cells through suppressing the PI3K-AKT pathway [101] resulting 49% of synovial sarcoma patients 12-week progression-free survival rate in phase 2 study [102] indicating good efficacy of applying target therapies in synovial sarcomas.

DOI:10.14753/SE.2014.1917

Our previous study also found overexpression of Her2/neu due to oncogene amplification, which presents in subsets of synovial sarcomas associated with better prognosis [29], indicating the feasibility for trastuzumab in suitable patient candidates. It also worth to mention that EZH2, as a highly expressed pro-oncogenic regulator and closely associates with SYT-SSX fusion protein; it may not only serve as a potential diagnostic marker but also an attractive candidate for the target therapy in synovial sarcomas. SYT-SSX closely collaborates with ATF2, TLE1, PcG and HDAC in the repression of the tumor suppressor gene *early growth response 1 (EGR1)*, which is one of the target genes of ATF2 [22]. Romidepsin (FK228), a HDAC inhibitor, probably acts through acetylating either SYT-SSX or TLE1; causing instability of the complex and further dissociates from each other lead to reactivaction of *EGR1*, and tumor shrinkage in a preclinical synovial sarcoma model **(Figure 16)** [49, 103].

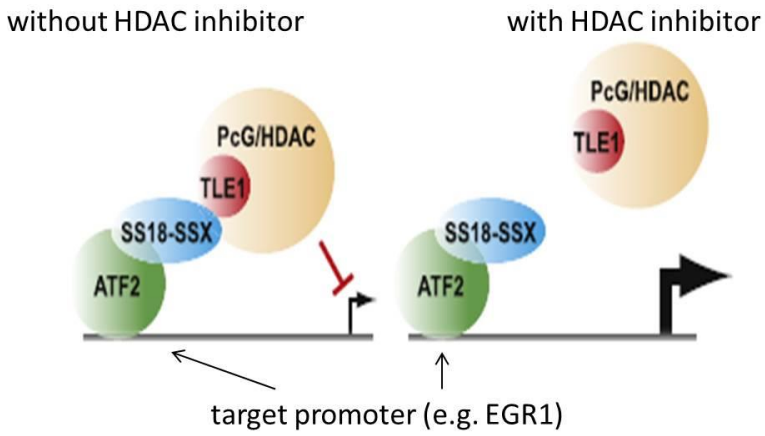

Figure 16. Illustration of the effect of HDAC inhibitor [49].

It is reasonable to assume that concomitant inhibition of HDAC and EZH2 might yield a synergistic effect. In vitro; successful repression of EZH2 was achieved by small interfering RNA (siRNA) as well as using the methyltransferase inhibitor 3-deazaneplanocin (DZNep) in human leukemic cells in culture which lead to depletion of PRC2, derepressed the target genes and apoptosis [104, 105]. It is crucial to know that due to the complexity of molecular crosstalk among the epigenetic regulation; the use of epigenetic drugs may result in a variety risk of unforeseeable effects, which limits the current clinical application of such therapies [106]. A recent-discovered drug, EZP-6439, an EZH2-specific inhibitor by competing its binding site with 5-adenosylmethionine showed a promising result in malignant rhabdoid tumor, which may represent a new potential treatment modality for synovial sarcomas [107].

Finally, the understanding of epigenetic (de)regulation of synovial sarcomas is a promising approach and the translations of these results into the diagnostic criteria and therapeutic strategies which may open novel treatment opportunities.

DOI:10.14753/SE.2014.1917

VI. Conclusions

Despite the controversies among the published data from the other groups; our investigations showed consistent association between DNA ploidy, karyotypic complexity and also the clinical outcome. Furthermore, study the epigenetic deregulation opens a new insight of oncogenesis of tumors; since EZH2 is a recently-discovered marker participating in tumor development in different type of cancers; its expression status and clinical relevance, particular in synovial sarcomas, are still largely unknown. We are the first group investigating EZH2 expression status and also the clinical relevance in synovial sarcoma at the present moment. We summarized our results as following:

1. Complex diploid group is associated with complex karyotype based on "single cell aneuploidy" phenomenon and has worse prognosis than simple diploid group.
2. EZH2 can serve as diagnostic adjunct since its expression helps to distinguish PDSS from the MPSS and BPSS. Its overexpression is also associated with unfavorable clinical outcome.
3. EZH2 expression correlates with H3K27me3 indicating functional participation of PRC2.
4. High EZH2 expression can be a predictive marker in terms of fast tumor growth rate and early development of metastasis which are particularly useful in MPSS and BPSS.
5. Both DNA ploidy and EZH2 expression have valuable prognostic impact in synovial sarcomas, since they offer complement data for clinicians in terms of patient management. EZH2 can also be the target for the epigenetic therapy, especially in combination with other epigenetic modulators and conventional chemotherapy to achieve maximized and synergetic effect.

DOI:10.14753/SE.2014.1917

VII. Summary

Synovial sarcoma is a high-grade malignant tumor of possibly mesenchymal stem cells origin with variable prognosis. Controversial data exist regarding ploidy, karyotype and clinical outcome. On the other hand; Enhancer of zeste homologue 2 (EZH2), the core member of polycomb repressing complex 2 (PRC2), showed overexpression in variable tumor types and its overexpression is associated with aggressive clinical course. However, its expression profile and clinical relevance in synovial sarcomas has little been discussed. We performed image cytometry with fine-tuned interpretation to 55 synovial sarcomas and correlated with the result of high-resolution comparative genomic hybridization (HR-CGH) and clinical outcome. Tissue microarray-based immunohistochemical study was also carried out to investigate the EZH2 expression among the histological subtypes, clinical data and patients' outcome. EZH2 expression was also measured at mRNA level by quantitative real-time PCR as well. Our results showed aneuploid, complex diploid and simple diploid DNA content are associated with particular karyotype complexity and prognosis. We also found high EZH2 expression preferentially aggregated in poorly differentiated synovial sarcomas. Cases with high EZH2 score, cross all subtypes, were associated with larger tumor size, early distant metastasis, and poor prognosis. Functional correlation between EZH2 and its epigenetic mark, H3K27me3, was also proved. We concluded both DNA ploidy and EZH2 expression possess valuable prognostic impacts in synovial sarcomas. They can be used as auxiliary diagnostic and prognostic tools, combined with morphology evaluation and the markers currently in used; which, in turn may help oncologists to select the appropriate therapy. EZH2 is also a potential therapeutic target in synovial sarcomas, especially when inhibited in combination with other epigenetic modulators to achieve synergistic therapeutic effect.

DOI:10.14753/SE.2014.1917

Összefoglalás

A synovialis sarcoma egy feltehetőleg mesenchymalis őssejt eredetű, magas grádusú, változó prognózisú rosszindulatú daganat. Ellentmondásos adatok állnak fent a ploiditás, a kariotípus és a klinikai kimenetel tekintetében. Az enhancer zeste homologue 2 (EZH2), a polycomb repressing complex 2 (PRC2) központi tagja, változó tumor típusokban kimutatható az overexpressziója, ami agresszív klinikai lefolyással jár. Ugyanakkor az EZH2 expressziós profilja és ennek a klinikai jelentősége synovialis sarcomában keveset tanulmányozott. Munkánk során 55 synovialis sarcoma mintán végeztünk képcitometriás vizsgálatot, és az így kapott eredményeket összevetettük a nagy felbontású komparatív genomiális hibridizációból (HR-CGH) származó eredményekkel, valamint a klinikai kimenetellel. Tissue microarray alapú immunhisztokémiai módszerrel vizsgáltuk az EZH2 expressziót a különböző szövettani altípusokban, betegcsoportokban és a klinikai adatok esetében. Az EZH2 expresszióját mRNS szinten is megmértük kvantitatív real-time PCR technikával. Vizsgálati eredményeink azt mutatták, hogy az aneuploid, a komplex diploid és az egyszerű diploid DNS tartalom sajátos kariotípus komplexitással és prognózissal jár együtt. Azt is megállapítottuk, hogy a magas EZH2 expresszió elsősorban a rosszul differenciált synovialis sarcomában fordul elő. A magas EZH2 score-ral rendelkező esetek nagyobb tumor mérettel, korai távoli metasztázis képződéssel és rossz prognózissal jellemezhetőek. Bizonyítást nyert az is, hogy funkcionális korreláció áll fent az EZH2 és annak epigenetikus markere, a H3K27me3 között. Arra a következtetésre jutottunk, hogy mind a DNS ploiditás, mind az EZH2 expresszió jelentős prognosztikai értékkel bírnak a synoviális sarcoma esetében. Ezért a jelenleg használt morfológiai értékelés és markerek mellett felhasználhatóak kiegészítő diagnosztikus és prognosztikus eszközökként, hogy az onkológusok segítségére legyenek a még megfelelőbb terápia

DOI:10.14753/SE.2014.1917

kialakításában. Az EZH2 ezen kívül potenciális terápiás célponttá is válhat a synovialis sarcomákban, különösen, amikor más epigenetikus modulátorokkal együtt gátolják a működését szinergetikus terápiás hatás elérése érdekében.

VIII. Bibliography

1. Naka N, Takenaka S, Araki N, Miwa T, Hashimoto N, Yoshioka K, Joyama S, Hamada K, Tsukamoto Y, Tomita Y, Ueda T, Yoshikawa H, Itoh K. (2010) Synovial sarcoma is a stem cell malignancy. Stem Cells, 28:1119-1131.
2. Fisher C dBD, Geurts van Kessel A. Synovial sarcoma. IARC Press, Lyon, 2002:23-215.
3. van de Rijn M, Barr FG, Xiong QB, Salhany KE, Fraker DL, Fisher C. (1997) Radiation-associated synovial sarcoma. Hum Pathol, 28:1325-1328.
4. Castañeda-Galindo LG, Castañeda-Leeder P, Lira-Puerto V. (2011) Synovial sarcoma in a patient with metal-on-polyethylene total hip replacement. A case report. Acta Ortop Mex, 25:242-245.
5. Enzinger FM, Weiss SW. Soft Tissue Tumors. Mosby, St. Louis, 2008:1161-1175.
6. Terry J, Saito T, Subramanian S, Ruttan C, Antonescu CR, Goldblum JR, Downs-Kelly E, Corless CL, Rubin BP, van de Rijn M, Ladanyi M, Nielsen TO. (2007) TLE1 as a diagnostic immunohistochemical marker for synovial sarcoma emerging from gene expression profiling studies. Am J Surg Pathol, 31:240-246.
7. Foo WC, Cruise MW, Wick MR, Hornick JL. (2011) Immunohistochemical staining for TLE1 distinguishes synovial sarcoma from histologic mimics. Am J Clin Pathol, 135:839-844.
8. Changchien YC, Katalin U, Fillinger J, Fónyad L, Papp G, Salamon F, Sápi Z. (2012) A challenging case of metastatic intra-abdominal synovial sarcoma with unusual immunophenotype and its differential diagnosis. Case Rep Pathol, 2012:786083.

9. Ladanyi M. (2001) Fusions of the SYT and SSX genes in synovial sarcoma. Oncogene, 20:5755-5762.

10. de Bruijn DRH, Nap JP, van Kessel AG. (2007) The (epi)genetics of human synovial sarcoma. Genes Chromosomes & Cancer, 46:107-117.

11. Haldar M, Randall RL, Capecchi MR. (2008) Synovial sarcoma: From genetics to genetic-based animal modeling. Clinical Orthopaedics and Related Research, 466:2156-2167.

12. Waterfall JJ, Meltzer PS. (2012) Targeting Epigenetic Misregulation in Synovial Sarcoma. Cancer Cell, 21:323-324.

13. Debernardi S, Bassini A, Jones LK, Chaplin T, Linder B, de Bruijn DR, Meese E, Young BD. (2002) The MLL fusion partner AF10 binds GAS41, a protein that interacts with the human SWI/SNF complex. Blood, 99:275-281.

14. Delattre O, Zucman J, Plougastel B, Desmaze C, Melot T, Peter M, Kovar H, Joubert I, de Jong P, Rouleau G. (1992) Gene fusion with an ETS DNA-binding domain caused by chromosome translocation in human tumours. Nature, 359:162-165.

15. Thaete C, Brett D, Monaghan P, Whitehouse S, Rennie G, Rayner E, Cooper CS, Goodwin G. (1999) Functional domains of the SYT and SYT-SSX synovial sarcoma translocation proteins and co-localization with the SNF protein BRM in the nucleus. Human Molecular Genetics, 8:585-591.

16. Nagai M, Tanaka S, Tsuda M, Endo S, Kato H, Sonobe H, Minami A, Hiraga H, Nishihara H, Sawa H, Nagashima K. (2001) Analysis of transforming activity of human synovial sarcoma-associated chimeric protein SYT-SSX1 bound to chromatin remodeling factor hBRM/hSNF2 alpha. Proceedings of the National Academy of Sciences of the United States of America, 98:3843-3848.

17. Margolin JF, Friedman JR, Meyer WK, Vissing H, Thiesen HJ, Rauscher FJ. (1994) Krüppel-associated boxes are potent transcriptional repression domains. Proc Natl Acad Sci U S A, 91:4509-4513.

18. Lim FL, Soulez M, Koczan D, Thiesen HJ, Knight JC. (1998) A KRAB-related domain and a novel transcription repression domain in proteins encoded by SSX genes that are disrupted in human sarcomas. Oncogene, 17:2013-2018.

19. Yamashita T, Agulnick AD, Copeland NG, Gilbert DJ, Jenkins NA, Westphal H. (1998) Genomic structure and chromosomal localization of the mouse LIM domain-binding protein 1 gene, Ldb1. Genomics, 48:87-92.

20. Naka N, Takenaka S, Araki N, Miwa T, Hashimoto N, Yoshioka K, Joyama S, Hamada KI, Tsukamoto Y, Tomita Y, Ueda T, Yoshikawa H, Itoh K. (2010) Synovial Sarcoma Is a Stem Cell Malignancy. Stem Cells, 28:1119-1131.

21. Sun B, Sun Y, Wang J, Zhao X, Zhang S, Liu Y, Li X, Feng Y, Zhou H, Hao X. (2008) The diagnostic value of SYT-SSX detected by reverse transcriptase-polymerase chain reaction (RT-PCR) and fluorescence in situ hybridization (FISH) for synovial sarcoma: a review and prospective study of 255 cases. Cancer Sci, 99:1355-1361.

22. Lubieniecka JM, de Bruijn DRH, Su L, van Dijk AHA, Subramanian S, van de Rijn M, Poulin N, van Kessel AG, Nielsen TO. (2008) Histone deacetylase inhibitors reverse SS18-SSX-mediated polycomb silencing of the tumor suppressor early growth response 1 in synovial sarcoma. Cancer Research, 68:4303-4310.

23. Kadoch C, Crabtree GR. (2013) Reversible Disruption of mSWI/SNF (BAF) Complexes by the SS18-SSX Oncogenic Fusion in Synovial Sarcoma. Cell, 153:71-85.

24. Svejstrup JQ. (2013) Synovial sarcoma mechanisms: a series of unfortunate events. Cell, 153:11-12.

25. Haldar M, Randall RL, Capecchi MR. (2008) Synovial sarcoma: from genetics to genetic-based animal modeling. Clin Orthop Relat Res, 466:2156-2167.

26. Villegas SN, Canham M, Brickman JM. (2010) FGF signalling as a mediator of lineage transitions--evidence from embryonic stem cell differentiation. J Cell Biochem, 110:10-20.

27. Garcia CB, Shaffer CM, Eid JE. (2012) Genome-wide recruitment to Polycomb-modified chromatin and activity regulation of the synovial sarcoma oncogene SYT-SSX2. BMC Genomics, 13:189.

28. Sun Y, Gao D, Liu Y, Huang J, Lessnick S, Tanaka S. (2006) IGF2 is critical for tumorigenesis by synovial sarcoma oncoprotein SYT-SSX1. Oncogene, 25:1042-1052.

29. Sápi Z, Pápai Z, Hruska A, Antal I, Bodó M, Orosz Z. (2005) Her-2 oncogene amplification, chromosome 17 and DNA ploidy status in synovial sarcoma. Pathol Oncol Res, 11:133-138.

30. Haldar M, Hancock JD, Coffin CM, Lessnick SL, Capecchi MR. (2007) A conditional mouse model of synovial sarcoma: insights into a myogenic origin. Cancer Cell, 11:375-388.

31. Xie YT, Skytting B, Nilsson G, Gasbarri A, Haslam K, Bartolazzi A, Brodin B, Mandahl N, Larsson O. (2002) SYT-SSX is critical for cyclin D1 expression in synovial sarcoma cells: A gain of function of the t(X;18)(p11.2;q11.2) translocation. Cancer Research, 62:3861-3867.

32. Cironi L, Provero P, Riggi N, Janiszewska M, Suva D, Suva ML, Kindler V, Stamenkovic I. (2009) Epigenetic Features of Human Mesenchymal Stem Cells Determine Their Permissiveness for Induction of Relevant Transcriptional Changes by SYT-SSX1. Plos One, 4:e7904.

33. Sauvageau M, Sauvageau G. (2010) Polycomb Group Proteins: Multi-Faceted Regulators of Somatic Stem Cells and Cancer. Cell Stem Cell, 7:299-313.

34. Surface LE, Thornton SR, Boyer LA. (2010) Polycomb Group Proteins Set the Stage for Early Lineage Commitment. Cell Stem Cell, 7:288-298.

35. Ciarapica R, Miele L, Giordano A, Locatelli F, Rota R. (2011) Enhancer of zeste homolog 2 (EZH2) in pediatric soft tissue sarcomas: first implications. Bmc Medicine, 9:63.

36. Woo CJ, Kharchenko PV, Daheron L, Park PJ, Kingston RE. (2010) A region of the human HOXD cluster that confers polycomb-group responsiveness. Cell, 140:99-110.

37. Rinn JL, Kertesz M, Wang JK, Squazzo SL, Xu X, Brugmann SA, Goodnough LH, Helms JA, Farnham PJ, Segal E, Chang HY. (2007) Functional demarcation of active and silent chromatin domains in human HOX loci by noncoding RNAs. Cell, 129:1311-1323.

38. Kanhere A, Viiri K, Araújo CC, Rasaiyaah J, Bouwman RD, Whyte WA, Pereira CF, Brookes E, Walker K, Bell GW, Pombo A, Fisher AG, Young RA, Jenner RG. (2010) Short RNAs are transcribed from repressed polycomb target genes and interact with polycomb repressive complex-2. Mol Cell, 38:675-688.

39. Peng JC, Valouev A, Swigut T, Zhang J, Zhao Y, Sidow A, Wysocka J. (2009) Jarid2/Jumonji coordinates control of PRC2 enzymatic activity and target gene occupancy in pluripotent cells. Cell, 139:1290-1302.

40. Schwartz YB, Kahn TG, Nix DA, Li XY, Bourgon R, Biggin M, Pirrotta V. (2006) Genome-wide analysis of Polycomb targets in Drosophila melanogaster. Nat Genet, 38:700-705.

41. Schoeftner S, Sengupta AK, Kubicek S, Mechtler K, Spahn L, Koseki H, Jenuwein T, Wutz A. (2006) Recruitment of PRC1 function at the initiation of X inactivation independent of PRC2 and silencing. EMBO J, 25:3110-3122.

42. Chase A, Cross NC. (2011) Aberrations of EZH2 in cancer. Clin Cancer Res, 17:2613-2618.

43. van der Vlag J, Otte AP. (1999) Transcriptional repression mediated by the human polycomb-group protein EED involves histone deacetylation. Nat Genet, 23:474-478.

44. Vire E, Brenner C, Deplus R, Blanchon L, Fraga M, Didelot C, Morey L, Van Eynde A, Bernard D, Vanderwinden JM, Bollen M, Esteller M, Di Croce L, de Launoit Y, Fuks F. (2007) The Polycomb group protein EZH2 directly controls DNA methylation (vol 439, pg 871, 2006). Nature, 446:824-824.

45. Li X, Gonzalez ME, Toy K, Filzen T, Merajver SD, Kleer CG. (2009) Targeted overexpression of EZH2 in the mammary gland disrupts ductal morphogenesis and causes epithelial hyperplasia. Am J Pathol, 175:1246-1254.

46. Chang CJ, Hung MC. (2012) The role of EZH2 in tumour progression. British Journal of Cancer, 106:243-247.

47. Hajósi-Kalcakosz S, Dezső K, Bugyik E, Bödör C, Paku S, Pávai Z, Halász J, Schlachter K, Schaff Z, Nagy P. (2012) Enhancer of zeste homologue 2 (EZH2) is a reliable immunohistochemical marker to differentiate malignant and benign hepatic tumors. Diagn Pathol, 7:86.

48. Shao Z, Raible F, Mollaaghababa R, Guyon JR, Wu CT, Bender W, Kingston RE. (1999) Stabilization of chromatin structure by PRC1, a Polycomb complex. Cell, 98:37-46.

49. Su L, Sampaio AV, Jones KB, Pacheco M, Goytain A, Lin SJ, Poulin N, Yi L, Rossi FM, Kast J, Capecchi MR, Underhil TM, Nielsen TO. (2012) Deconstruction of the SS18-SSX Fusion Oncoprotein Complex: Insights into Disease Etiology and Therapeutics. Cancer Cell, 21:333-347.

50. Haldar M, Hedberg ML, Hockin MF, Capecchi MR. (2009) A CreER-based random induction strategy for modeling translocation-associated sarcomas in mice. Cancer Res, 69:3657-3664.

51. Hayakawa K, Ikeya M, Fukuta M, Woltjen K, Tamaki S, Takahara N, Kato T, Sato S, Otsuka T, Toguchida J. (2013) Identification of target genes of synovial sarcoma-associated fusion oncoprotein using human pluripotent stem cells. Biochem Biophys Res Commun, 432(4):713-9.

52. Rodríguez R, García-Castro J, Trigueros C, García Arranz M, Menéndez P. (2012) Multipotent mesenchymal stromal cells: clinical applications and cancer modeling. Adv Exp Med Biol, 741:187-205.

53. Rubio R, Gutierrez-Aranda I, Sáez-Castillo AI, Labarga A, Rosu-Myles M, Gonzalez-Garcia S, Toribio ML, Menendez P, Rodriguez R. (2013) The differentiation stage of p53-Rb-deficient bone marrow mesenchymal stem cells imposes the phenotype of in vivo sarcoma development. Oncogene, 32(41):4970-80.

54. Lin PP, Pandey MK, Jin F, Raymond AK, Akiyama H, Lozano G. (2009) Targeted mutation of p53 and Rb in mesenchymal cells of the limb bud produces sarcomas in mice. Carcinogenesis, 30:1789-1795.

55. Nakagawa Y, Numoto K, Yoshida A, Kunisada T, Ohata H, Takeda K, Wai D, Poremba C, Ozaki T. (2006) Chromosomal and genetic imbalances in synovial sarcoma detected by conventional and microarray comparative genomic hybridization. J Cancer Res Clin Oncol, 132:444-450.

56. Randall RL, Schabel KL, Hitchcock Y, Joyner DE, Albritton KH. (2005) Diagnosis and management of synovial sarcoma. Curr Treat Options Oncol, 6:449-459.

57. Spurrell EL, Fisher C, Thomas JM, Judson IR. (2005) Prognostic factors in advanced synovial sarcoma: an analysis of 104 patients treated at the Royal Marsden Hospital. Ann Oncol, 16:437-444.

58. Okcu MF, Despa S, Choroszy M, Berrak SG, Cangir A, Jaffe N, Raney RB. (2001) Synovial sarcoma in children and adolescents: thirty three years of experience with multimodal therapy. Med Pediatr Oncol, 37:90-96.

59. Okcu MF, Munsell M, Treuner J, Mattke A, Pappo A, Cain A, Ferrari A, Casanova M, Ozkan A, Raney B. (2003) Synovial sarcoma of childhood and adolescence: a multicenter, multivariate analysis of outcome. J Clin Oncol, 21:1602-1611.

60. Ganjoo KN. (2010) New developments in targeted therapy for soft tissue sarcoma. Curr Oncol Rep, 12:261-265.

61. Lopes JM, Hannisdal E, Bjerkehagen B, Bruland OS, Danielsen HE, Pettersen EO, Sobrinho-Simões M, Nesland JM. (1998) Synovial sarcoma. Evaluation of prognosis with emphasis on the study of DNA ploidy and proliferation (PCNA and Ki-67) markers. Anal Cell Pathol, 16:45-62.

62. Skytting BT, Szymanska J, Aalto Y, Lushnikova T, Blomqvist C, Elomaa I, Larsson O, Knuutila S. (1999) Clinical importance of genomic imbalances in synovial sarcoma evaluated by comparative genomic hybridization. Cancer Genet Cytogenet, 115:39-46.

63. Yamaga K, Osaki M, Kidani K, Shomori K, Yoshida H, Ito H. (2008) High expression of enhancer of zeste homologue 2 indicates poor prognosis in patients with soft tissue sarcomas. Molecular Medicine Reports, 1:633-639.

64. Haroske G, Baak JPA, Danielsen H, Giroud F, Gschwendtner A, Oberholzer M, Reith A, Spieler P, Bocking A. (2001) Fourth updated ESACP consensus report on diagnostic DNA image cytometry. Analytical Cellular Pathology, 23:89-95.

65. Krause FS, Feil G, Bichler KH, Schrott KM, Akcetin ZY. (2003) Clinical aspects for the use of DNA image cytometry in detection of bladder cancer: a valuable tool? DNA Cell Biol, 22:721-725.

66. Miller SA, Dykes DD, Polesky HF. (1988) A simple salting out procedure for extracting DNA from human nucleated cells. Nucleic Acids Res, 16:1215.

67. Kallioniemi A, Kallioniemi OP, Sudar D, Rutovitz D, Gray JW, Waldman F, Pinkel D. (1992) Comparative genomic hybridization for molecular cytogenetic analysis of solid tumors. Science, 258:818-821.

68. Kirchhoff M, Gerdes T, Rose H, Maahr J, Ottesen AM, Lundsteen C. (1998) Detection of chromosomal gains and losses in comparative genomic hybridization analysis based on standard reference intervals. Cytometry, 31:163-173.

69. Brassesco MS, Cortez MA, Valera ET, Engel EE, Nogueira-Barbosa MH, Becker AP, Tone LG. (2010) Cytogenetic heterogeneity in biphasic synovial sarcoma associated with telomere instability. Cancer Genet Cytogenet, 197:86-90.

70. Chatelain R, Schunck T, Schindler EM, Schindler AE, Böcking A. (1989) Diagnosis of prospective malignancy in koilocytic dysplasias of the cervix with DNA cytometry. J Reprod Med, 34:505-510.

71. Nakayama R, Mitani S, Nakagawa T, Hasegawa T, Kawai A, Morioka H, Yabe H, Toyama Y, Ogose A, Toguchida J, Nakayama T, Yoshida T, Ichikawa H. (2010) Gene Expression Profiling of Synovial Sarcoma: Distinct Signature of Poorly Differentiated Type. American Journal of Surgical Pathology, 34:1599-1607.

72. Koh CM, Iwata T, Zheng QZ, Bethel C, Yegnasubramanian S, De Marzo AM. (2011) Myc Enforces Overexpression of EZH2 in Early Prostatic Neoplasia via Transcriptional and Post-transcriptional Mechanisms. Oncotarget, 2:669-683.

73. Ciarapica R, Russo G, Verginelli F, Raimondi L, Donfrancesco A, Rota R, Giordano A. (2009) Deregulated expression of miR-26a and Ezh2 in rhabdomyosarcoma. Cell Cycle, 8:172-175.

74. Chang CJ, Yang JY, Xia W, Chen CT, Xie X, Chao CH, Woodward WA, Hsu JM, Hortobagyi GN, Hung MC. (2011) EZH2 promotes expansion of breast tumor initiating cells through activation of RAF1-β-catenin signaling. Cancer Cell, 19:86-100.

75. Richter GHS, Plehm S, Fasan A, Rossler S, Unland R, Bennani-Baiti IM, Hotfilder M, Lowel D, von Luettichau I, Mossbrugger I, Quintanilla-Martinez L, Kovar H, Staege MS, Muller-Tidow C, Burdach S. (2009) EZH2 is a mediator of EWS/FLI1 driven tumor growth and metastasis blocking endothelial and neuro-ectodermal differentiation. Proceedings of the National Academy of Sciences of the United States of America, 106:5324-5329.

76. Varambally S, Dhanasekaran SM, Zhou M, Barrette TR, Kumar-Sinha C, Sanda MG, Ghosh D, Pienta KJ, Sewalt R, Otte AP, Rubin MA, Chinnaiyan AM. (2002) The polycomb group protein EZH2 is involved in progression of prostate cancer. Nature, 419:624-629.

77. Yu J, Rhodes DR, Tomlins SA, Cao X, Chen G, Mehra R, Wang X, Ghosh D, Shah RB, Varambally S, Pienta KJ, Chinniaiyan AM. (2007) A polycomb repression signature in metastatic prostate cancer predicts cancer outcome. Cancer Research, 67:10657-10663.

78. Bracken AP, Pasini D, Capra M, Prosperini E, Colli E, Helin K. (2003) EZH2 is downstream of the pRB-E2F pathway, essential for proliferation and amplified in cancer. EMBO J, 22:5323-5335.

79. Wu ZL, Zheng SS, Li ZM, Qiao YY, Aau MY, Yu Q. (2010) Polycomb protein EZH2 regulates E2F1-dependent apoptosis through epigenetically modulating Bim expression. Cell Death Differ, 17:801-810.

80. Cao Q, Yu J, Dhanasekaran SM, Kim JH, Mani RS, Tomlins SA, Mehra R, Laxman B, Cao X, Kleer CG, Varambally S, Chinnaiyan AM. (2008) Repression of E-cadherin by the polycomb group protein EZH2 in cancer. Oncogene, 27:7274-7284.

81. Lu C, Han HD, Mangala LS, Ali-Fehmi R, Newton CS, Ozbun L, Armaiz-Pena GN, Hu W, Stone RL, Munkarah A, Ravoori MK, Shahzad MM, Lee JW, Mora E, Langley RR, Carroll AR, Matsuo K, Spannuth WA, Schmandt R, Jennings NB, Goodman BW, Jaffe RB, Nick AM, Kim HS, Guven EO, Chen YH, Li LY, Hsu MC, Coleman RL, Calin GA, Denkbas EB, Lim JY, Lee JS, Kundra V, Birrer MJ, Hung MC, Lopez-Berestein G, Sood AK. (2010) Regulation of tumor angiogenesis by EZH2. Cancer Cell, 18:185-197.

82. Barco R, Garcia CB, Eid JE. (2009) The Synovial Sarcoma-Associated SYT-SSX2 Oncogene Antagonizes the Polycomb Complex Protein Bmi1. Plos One, 4.

83. Piunti A, Pasini D. (2011) Epigenetic factors in cancer development: Polycomb group proteins. Future Oncology, 7:57-75.

84. Yap DB, Chu J, Berg T, Schapira M, Cheng SW, Moradian A, Morin RD, Mungall AJ, Meissner B, Boyle M, Marquez VE, Marra MA, Gascoyne RD, Humphries RK, Arrowsmith CH, Morin GB, Aparicio SA. (2011) Somatic mutations at EZH2 Y641 act dominantly through a mechanism of selectively altered PRC2 catalytic activity, to increase H3K27 trimethylation. Blood, 117:2451-2459.

85. Bödör C, O'Riain C, Wrench D, Matthews J, Iyengar S, Tayyib H, Calaminici M, Clear A, Iqbal S, Quentmeier H, Drexler HG, Montoto S, Lister AT, Gribben JG, Matolcsy A, Fitzgibbon J. (2011) EZH2 Y641 mutations in follicular lymphoma. Leukemia, 25:726-729.

86. Cai MY, Hou JH, Rao HL, Luo RZ, Li M, Pei XQ, Lin MC, Guan XY, Kung HF, Zeng YX, Xie D. (2011) High expression of H3K27me3 in human hepatocellular carcinomas correlates closely with vascular invasion and predicts worse prognosis in patients. Mol Med, 17:12-20.

87. He LR, Liu MZ, Li BK, Rao HL, Liao YJ, Guan XY, Zeng YX, Xie D. (2009) Prognostic impact of H3K27me3 expression on locoregional progression after chemoradiotherapy in esophageal squamous cell carcinoma. BMC Cancer, 9:461.

88. Wei Y, Xia W, Zhang Z, Liu J, Wang H, Adsay NV, Albarracin C, Yu D, Abbruzzese JL, Mills GB, Bast RC, Hortobagyi GN, Hung MC. (2008) Loss of trimethylation at lysine 27 of histone H3 is a predictor of poor outcome in breast, ovarian, and pancreatic cancers. Mol Carcinog, 47:701-706.

89. Kuzmichev A, Margueron R, Vaquero A, Preissner TS, Scher M, Kirmizis A, Ouyang X, Brockdorff N, Abate-Shen C, Farnham P, Reinberg D. (2005) Composition and histone substrates of polycomb repressive group complexes change during cellular differentiation. Proc Natl Acad Sci U S A, 102:1859-1864.

90. Cha TL, Zhou BP, Xia W, Wu Y, Yang CC, Chen CT, Ping B, Otte AP, Hung MC. (2005) Akt-mediated phosphorylation of EZH2 suppresses methylation of lysine 27 in histone H3. Science, 310:306-310.

91. Kuzmichev A, Margueron R, Vaquero A, Preissner TS, Scher M, Kirmizis A, Ougang XS, Brockdorff N, Abate-Shen C, Farnham P, Reinberg D. (2005) Composition and histone substrates of polycomb repressive group complexes change during cellular differentiation. Proceedings of the National Academy of Sciences of the United States of America, 102:1859-1864.

92. Chen S, Bohrer LR, Rai AN, Pan Y, Gan L, Zhou X, Bagchi A, Simon JA, Huang H. (2010) Cyclin-dependent kinases regulate epigenetic gene silencing through phosphorylation of EZH2. Nat Cell Biol, 12:1108-1114.

93. Wei Y, Chen YH, Li LY, Lang J, Yeh SP, Shi B, Yang CC, Yang JY, Lin CY, Lai CC, Hung MC. (2011) CDK1-dependent phosphorylation of EZH2 suppresses methylation of H3K27 and promotes osteogenic differentiation of human mesenchymal stem cells. Nat Cell Biol, 13:87-94.

94. Wu SC, Zhang Y. (2011) Cyclin-dependent kinase 1 (CDK1)-mediated phosphorylation of enhancer of zeste 2 (Ezh2) regulates its stability. J Biol Chem, 286:28511-28519.

95. Hasegawa T, Yamamoto S, Yokoyama R, Umeda T, Matsuno Y, Hirohashi S. (2002) Prognostic significance of grading and staging systems using MIB-1 score in adult patients with soft tissue sarcoma of the extremities and trunk. Cancer, 95:843-851.

96. Balogh Z, Szemlaky Z, Szendroi M, Antal I, Pápai Z, Fónyad L, Papp G, Changchien YC, Sápi Z. (2011) Correlation between DNA ploidy, metaphase high-resolution comparative genomic hybridization results and clinical outcome of synovial sarcoma. Diagn Pathol, 6:107.

97. Blay JY, Ray-Coquard I, Alberti L, Ranchère D: Targeting other abnormal signaling pathways in sarcoma: EGFR in synovial sarcomas, PPAR-gamma in liposarcomas. Cancer Treat Res 2004, 120:151-167.

98. Joyner DE, Albritton KH, Bastar JD, Randall RL. (2006) G3139 antisense oligonucleotide directed against antiapoptotic Bcl-2 enhances doxorubicin cytotoxicity in the FU-SY-1 synovial sarcoma cell line. J Orthop Res, 24:474-480.

99. Kim R, Emi M, Matsuura K, Tanabe K. (2007) Antisense and nonantisense effects of antisense Bcl-2 on multiple roles of Bcl-2 as a chemosensitizer in cancer therapy. Cancer Gene Ther, 14:1-11.

100. Jones KB, Su L, Jin H, Lenz C, Randall RL, Underhill TM, Nielsen TO, Sharma S, Capecchi MR. (2013) SS18-SSX2 and the mitochondrial apoptosis pathway in mouse and human synovial sarcomas. Oncogene, 32(18):2365-71.

101. Hosaka S, Horiuchi K, Yoda M, Nakayama R, Tohmonda T, Susa M, Nakamura M, Chiba K, Toyama Y, Morioka H. (2012) A novel multi-kinase inhibitor pazopanib suppresses growth of synovial sarcoma cells through inhibition of the PI3K-AKT pathway. J Orthop Res, 30:1493-1498.

102. Sleijfer S, Ray-Coquard I, Papai Z, Le Cesne A, Scurr M, Schöffski P, Collin F, Pandite L, Marreaud S, De Brauwer A, van Glabbeke M, Verweij J, Blay JY. (2009) Pazopanib, a multikinase angiogenesis inhibitor, in patients with relapsed or refractory advanced soft tissue sarcoma: a phase II study from the European organisation for research and treatment of cancer-soft tissue and bone sarcoma group (EORTC study 62043). J Clin Oncol, 27:3126-3132.

103. Ito T, Ouchida M, Morimoto Y, Yoshida A, Jitsumori Y, Ozaki T, Sonobe H, Inoue H, Shimizu K. (2005) Significant growth suppression of synovial sarcomas by the histone deacetylase inhibitor FK228 in vitro and in vivo. Cancer Lett, 224:311-319.

104. Tan J, Yang X, Zhuang L, Jiang X, Chen W, Lee PL, Karuturi RK, Tan PB, Liu ET, Yu Q. (2007) Pharmacologic disruption of Polycomb-repressive complex 2-mediated gene repression selectively induces apoptosis in cancer cells. Genes Dev, 21:1050-1063.

105. Fiskus W, Wang Y, Sreekumar A, Buckley KM, Shi H, Jillella A, Ustun C, Rao R, Fernandez P, Chen J, Balusu R, Koul S, Atadja P, Marquez VE, Bhalla KN. (2009) Combined epigenetic therapy with the histone methyltransferase EZH2 inhibitor 3-deazaneplanocin A and the histone deacetylase inhibitor panobinostat against human AML cells. Blood, 114:2733-2743.

106. Wang C, Liu Z, Woo CW, Li Z, Wang L, Wei JS, Marquez VE, Bates SE, Jin Q, Khan J, Ge K, Thiele CJ. (2012) EZH2 Mediates epigenetic silencing of neuroblastoma suppressor genes CASZ1, CLU, RUNX3, and NGFR. Cancer Res, 72:315-324.

107. Knutson SK, Warholic NM, Wigle TJ, Klaus CR, Allain CJ, Raimondi A, Porter Scott M, Chesworth R, Moyer MP, Copeland RA, Richon VM, Pollock RM, Kuntz KW, Keilhack H. (2013) Durable tumor regression in genetically altered malignant rhabdoid tumors by inhibition of methyltransferase EZH2. Proc Natl Acad Sci U S A, 110:7922-7927.

DOI:10.14753/SE.2014.1917

IX. Publication records

IX.1 Publications related to the theme

1. Changchien YC, Tátrai P, Papp G, Sápi J, Fónyad L, Szendrői M, Pápai Z, Sápi Z. (2012) Poorly differentiated synovial sarcoma is associated with high expression of enhancer of zeste homologue 2 (EZH2). J Transl Med, Oct 30;10:216.

IF:3,47

2. Balogh Z, Szemlaky Z, Szendroi M, Antal I, Pápai Z, Fónyad L, Papp G, Changchien YC, Sápi Z. (2011) Correlation between DNA ploidy, metaphase high-resolution comparative genomic hybridization results and clinical outcome of synovial sarcoma. Diagn Pathol, Nov 3;6:107.

IF:1,64

3. Changchien YC, Katalin U, Fillinger J, Fónyad L, Papp G, Salamon F, Sápi Z. (2012) A challenging case of metastatic intra-abdominal synovial sarcoma with unusual immunophenotype and its differential diagnosis. Case Rep Pathol, 2012:786083.

IX.2 Publications not related to the theme

1. Papp G, Changchien YC, Péterfia B, Pecsenka L, Krausz T, Stricker TP, Khoor A, Donner L, Sápi Z. (2013) SMARCB1 protein and mRNA loss is not caused by promoter and histone hypermethylation in epithelioid sarcoma. Mod Pathol, Mar;26(3):393-403.
IF: 4,792

2. Changchien YC, Haltrich I, Micsik T, Kiss E, Fónyad L, Papp G, Sápi Z. (2012) Gonadoblastoma: Case report of two young patients with isochromosome 12p found in the dysgerminoma overgrowth component in one case. Pathol Res Pract, Oct 15;208(10):628-32.
IF: 1,213

DOI:10.14753/SE.2014.1917

X. Acknowledgements

First of all, I would like to thank of gratitude to my supervisor Professor Zoltán Sápi, from the 1st Department of Pathology and Experimental Cancer research, Semmelweis University for the opportunity to perform my PhD work in my favorite field of soft tissue pathology, and also for his help and support during my research work and teach me soft tissue pathology.

I also would like to thank Professor András Matolcsy, the leader of the department for giving me the precious opportunity to do this wonderful project.

I am very grateful to Professor Ilona Kovalszky for allowing me using the delicated biochemical instrutments and the colleagues for teaching everything I need to know for my research.

I would like to express my special thanks to my colleagues, Dr. Gergő Papp from 1st department of pathology and experimental cancer research, Semmelweis University, and Dr. Peter Tatrai from Creative Cell Lab., Budapest, who gave me tons of technical assistance and rigorously reviewed my pre-submitted manuscripts. These have made me came to know about so many new things.

I also would like to show my appreciation to the Prof. Miklós Szendrői and Dr. Tamás Terebessy from the orthopedic department of Semmelweis University for the research material contributions.

I am deeply thankful to Ilona Polgár for her professional microtome skill and everyone in the 1st department of pathology and experimental cancer research, Semmelweis University who ever helped me from “bedside back to the bench” and also for the language assistance.

I also would like to thank my resident colleagues in the department for giving me the opportunity to review and refresh my pathology knowledge beside the research

DOI:10.14753/SE.2014.1917

work.

Last but not the least; I would like to thank my wife, Dr. Mariann Pintye and my families for their continuous support and sacrifice.

I made this project not only for the personal interests, but to also increase my knowledge in basic biomedical science what a practicing pathologist should equip. I would like to thank again to all who helped me.